NIH-PA Author Manuscript

Age-related loss of phospholipid asymmetry in APP^{NLh}/APP^{NLh} × PS-1^{P264L}/PS-1^{P264L} human double knock-in mice: Relevance to Alzheimer disease

Miranda L. Bader Lange[a,b], **Daret St. Clair**[c], **William R. Markesbery**[d,e], **Christa M. Studzinski**[d], **M. Paul Murphy**[d,f], and **D. Allan Butterfield**[a,b,d,*]

[a]Department of Chemistry, University of Kentucky, Lexington, KY 40506, USA

[b]Center of Membrane Sciences, University of Kentucky, Lexington, KY 40506, USA

[c]Graduate Center for Toxicology, University of Kentucky, Lexington, KY 40536, USA

[d]Sanders-Brown Center on Aging, University of Kentucky, Lexington, KY 40536, USA

[e]Department of Pathology and Neurology, University of Kentucky, Lexington, KY 40536, USA

[f]Department of Molecular and Cellular Biochemistry, University of Kentucky, Lexington, KY 40536, USA

Abstract

Using APP^{NLh}/APP^{NLh}×PS-1^{P246L}/PS-1^{P246L} human double knock-in (APP/PS-1) mice, we examined whether phosphatidylserine (PtdSer) asymmetry is significantly altered in brain of this familial Alzheimer disease mouse model in an age-dependent manner as a result of oxidative stress, toxic $A\beta(1\text{--}42)$ oligomer production, and/or apoptosis. Annexin V (AV) and NBD-PS fluorescence in synaptosomes of wild-type (WT) and APP/PS-1 mice were used to determine PtdSer exposure with age, while Mg^{2+}ATPase activity was determined to correlate PtdSer asymmetry changes with PtdSer translocase, flippase, activity. AV and NBD-PS results demonstrated significant PtdSer exposure beginning at 9 months compared to 1 month-old WT controls for both assays, a trend that was exacerbated in synaptosomes of APP/PS-1 mice. Decreasing Mg^{2+}ATPase activity confirms that the age-related loss of PtdSer asymmetry is likely due to loss of flippase activity, more prominent in APP/PS-1 brain. Two-site sandwich ELISA on SDS- and FA-soluble APP/PS-1 brain fractions were conducted to correlate $A\beta(1\text{--}40)$ and $A\beta(1\text{--}42)$ levels with age-related trends determined from the AV, NBD-PS, and Mg^{2+}ATPase assays. ELISA revealed a significant increase in both SDS- and FA-soluble $A\beta(1\text{--}40)$ and $A\beta(1\text{--}42)$ with age, consistent with PtdSer and flippase assay trends. Lastly, because PtdSer exposure is affected by pro-apoptotic caspase-3, levels of both latent and active forms were measured. Western blotting results demonstrated an increase in both active fragments of caspase-3 with age, while levels of pro-caspase-3 decrease. These results are discussed with relevance to loss of lipid asymmetry and consequent neurotoxicity in brain of subjects with Alzheimer disease.

*Address correspondence to: Professor D. Allan Butterfield, Department of Chemistry, Center of Membrane Sciences, and Sanders-Brown Center on Aging, University of Kentucky, Lexington, KY 40506-0055, USA, Tel: 1 - (859) 257-3184, Fax: 1 - (859) 257-5876, dabcns@uky.edu.

Publisher's Disclaimer: This is a PDF file of an unedited manuscript that has been accepted for publication. As a service to our customers we are providing this early version of the manuscript. The manuscript will undergo copyediting, typesetting, and review of the resulting proof before it is published in its final citable form. Please note that during the production process errors may be discovered which could affect the content, and all legal disclaimers that apply to the journal pertain.

Keywords

Amyloid precursor protein (APP); presenilin-1 (PS-1); familial Alzheimer disease (FAD); phosphatidylserine (PtdSer); phospholipid asymmetry; oxidative stress; lipid peroxidation; toxic Aβ(1–42) oligomers; apoptosis; caspase-3

Introduction

Alzheimer disease (AD) is an age-associated neurodegenerative disorder characterized by synapse and neuronal cell loss, as well as appearance of neurofibrillary tangles and neuritic plaques. Familial Alzheimer disease (FAD) is caused by autosomal dominant mutations in the amyloid precursor protein (APP) or presenilin (PS) genes 1 and 2 (Citron et al., 1992; Scheuner et al., 1996; Sturchler-Pierrat et al., 1997), a mutation in PS-1 being more aggressive. Since presenilins regulate processing of APP (Selkoe et al., 1996), mutations in APP and PS-1 or PS-2 result in the increased production of pathologic Aβ(1–42) (Borchelt et al., 1997; Cai et al., 1993; Oyama et al., 1998; Scheuner et al., 1996), which rapidly oligomerizes, aggregates into fibrils, and finally deposits as the main component of neuritic plaques (Selkoe, 2001; Wirths et al., 2006). However, it is the longer, more hydrophobic Aβ(1–42) that is toxic in AD (Drake et al., 2003; Lambert et al., 1998; Mattson, 1997), as it is considerably more prone to oligomerization and subsequent fibril formation than the more abundantly produced Aβ(1–40) (Burdick et al., 1992; Jarrett et al., 1993).

Oxidative stress induced lipid peroxidation in AD and FAD disrupts cellular homeostasis (Butterfield and Lauderback, 2002; Lauderback et al., 2001), such as loss of membrane asymmetry (Bader Lange et al., 2008; Castegna et al., 2004; Mohmmad Abdul and Butterfield, 2005). Normally, the aminophospholipid phosphatidylserine (PtdSer) is sequestered to the inner leaflet of the plasma membrane (Daleke and Lyles, 2000; Daleke, 2003; Paulusma and Oude Elferink, 2005). However, asymmetric collapse induced by lipid peroxidation products, such as 4-hydroxy-2-nonenal (HNE) and acrolein (Butterfield et al., 2006; Lauderback et al., 2001; Lovell et al., 2001; Markesbery and Lovell, 1998), exposes PtdSer to the outer leaflet signaling the first stages of an apoptotic process (Bader Lange et al., 2008; Fadok et al., 1992; Kagan et al., 2003; Tyurina et al., 2004).

Likewise, toxic Aβ(1–42) oligomers can initiate lipid peroxidation events during AD progression (Butterfield et al., 2002; 2007; Lambert et al., 1998; Schubert et al., 1995; Selkoe, 2001) by membrane integration and/or surface binding (Hertel et al., 1997; Kayed et al., 2004; McLaurin and Chakrabartty, 1997). Oligomer-induced peroxidation has the potential to disrupt phosphatidylinositol-4,5-bisphosphate metabolism (Berman et al., 2008), increase bilayer conductance through alteration of dielectric structure (Sokolov et al., 2006), and increase bilayer permeability (Arispe and Doh, 2002; Demuro et al., 2005; Kayed et al., 2004; Muller et al., 1995). Moreover, phospholipids have also been shown to stabilize toxic oligomers generated from monomeric Aβ (Johansson et al., 2007; Martins et al., 2008). Consequently, oligomeric Aβ(1–42) could be a major contributor to oxidative damage observed in AD and FAD by augmenting lipid peroxidation, indexed by elevated levels of highly reactive HNE and acrolein, subsequently disrupting PtdSer distribution.

Aβ-induced oxidative stress can also result in increased pro-apoptotic factor expression, effectively elevating the levels of apoptosis and neuronal cell death. In particular, activated aspartate-specific cysteine protease-3 (caspase-3) immunoreactivity has been shown to be elevated in neurons and astrocytes of subjects with AD (Su et al., 2001). Moreover, PtdSer exposure and loss of flippase activity is noted to occur downstream of caspase-3 activation in some non-neuronal cell types (Mandal et al., 2002; Mandal et al., 2005; Martin et al., 1996;

Vanags et al., 1996). Therefore, PtdSer externalization could be the result of one or more factors in the brain either working alone or in concert to affect cellular homeostasis.

In brain of $APP^{NLh}/APP^{NLh} \times PS-1^{P246L}/PS-1^{P246L}$ double knock-in mice (APP/PS-1), Aβ(1–42) deposition is observed in an age-dependent manner beginning at 9 months, with neuritic plaques developing at 12 months of age (Anantharaman et al., 2006; Reaume et al., 1996; Siman et al., 2000). In the present study, PtdSer asymmetry in synaptosomes prepared from brain isolated from wild-type and APP/PS-1 mice was examined in an age-dependent manner using Annexin V (AV) and NBD-PS fluorescent assays (Bader Lange et al., 2008) to test the hypothesis that PtdSer asymmetry is significantly altered in the brain of this FAD mouse model, in parallel with significantly elevated Aβ(1–42) levels. In addition, Mg^{2+}ATPase activity was determined to correlate PtdSer asymmetry changes with PtdSer translocase, flippase, activity, while Western blotting was employed to investigate how PtdSer asymmetry and flippase activity is affected by the levels of pro-apoptotic caspase-3. Two-site sandwich ELISA on SDS- and FA-soluble brain fractions of APP/PS-1 mice was conducted in order to correlate soluble Aβ(1–40) and Aβ(1–42) levels with possible age-related trends ascertained from the AV, NBD-PS, and Mg^{2+}ATPase assays.

Materials & Methods

All chemicals and antibodies used in ELISA, lipid asymmetry, and Mg^{2+}ATPase studies were purchased from Sigma-Aldrich (St. Louis, MO) with the exceptions of Annexin V FITC obtained from Invitrogen Molecular Probes (Eugene, OR), NBD-PS [1-palmitoyl-2-[6(7-nitrobenz-2-oxa-1,3-diazol-4-yl)amino]caproyl-*sn*-glycero-3-phosphoserine] obtained from Avanti Polar Lipids (Alabaster, AL), TMB reagent obtained from Kirkegaard and Perry Laboratories (Gaithersburg, MD), and Block Ace solution from Serotec (Raleigh, NC). The primary antibody for caspase-3 was purchased from Calbiochem (La Jolla, CA), while the primary antibody for α-tubulin was purchased from Sigma-Aldrich (St. Louis, MO). Both Amersham ECL-HRP linked anti-mouse and anti-rabbit secondary antibodies, as well as Amersham ECL-Plus Western blotting detection reagents were purchased from GE Healthcare (Pittsburgh, PA). Criterion precast polyacrylamide gels, XT MES running buffer, and nitrocellulose membranes were purchased from Bio-RAD (Hercules, CA).

APP/PS-1 mice

The University of Kentucky Animal Care and Use Committee approved all procedures used in this study. Mice used in this study were male $APP^{NLh}/APP^{NLh} \times PS-1^{P264L}/PS-1^{P264L}$ human double knock-in generated using Cre-loc© knock-in technology (Cephalon, Inc., Westchester, PA) to humanize the mouse Aβ sequence (NLh) and create a PS-1 proline to leucine mutation on codon 264 (P264L), identified in human FAD (Reaume et al., 1996; Siman et al., 2000). These double knock-in mice yield proper cleavage of the APP protein to generate Aβ. Gene expression produced by crossing APP (NLh) and PS-1 (P264L) knock-in mice is driven by endogenous promoters of the APP and PS-1 genes; therefore, expression is limited by replacement of these genes and not by expression of multiple transgenes (Anantharaman et al., 2006). Wild-type (WT) and APP/PS-1 mouse age groups used in this study were 1, 3, 6, 9, and 12 months-old. Whole brain tissue was extracted and frozen at −80 °C until used.

Measurement of Aβ solubility by sandwich ELISA

The solubility of Aβ was measured by a standard three-step serial extraction, as described previously (Das et al., 2003; Kukar et al., 2005; McGowan et al., 2005; Murphy et al., 2007). Briefly, brain tissue was homogenized in a polytron homogenizer in DEA buffer (50 mM NaCl, 0.2% diethylamine, 1.0 ml/150 mg tissue) including a complete protease inhibitor cocktail. Samples were centrifuged at $14,000 \times g$ for 30 min at 4 °C, and the supernatant collected. The

pellet was re-extracted by sonication (10×0.5 s microtip pulses at 100 W; Fisher Sonic Dismembrator, Model 500) in 2% SDS and centrifuged at $14,000 \times g$ for 30 min at room temperature. The supernatant was again collected, and the remaining pellet was extracted by sonication in 70% formic acid (FA) and centrifuged at $100,000 \times g$ for 1 h in a Beckman OptimaMAX tabletop ultracentrifuge (TLA55 rotor; Fullerton, CA). Sample extracts were then stored at −80 °C until the time of ELISA assay.

Thawed SDS-soluble fractions were diluted in AC buffer (0.02 M sodium phosphate buffer (pH 7), 0.4 M NaCl, 2 mM EDTA, 0.4% Block Ace, 0.2% BSA, 0.05% CHAPS, and 0.05% NaN_3), while FA fractions were diluted in AC buffer following neutralization by 1:20 dilution in TP buffer (1 M Tris base, 0.5 M Na_2HPO_4). Pilot studies were completed to empirically determine final sample dilutions. Aβ(1–40) and Aβ(1–42) standard curves were prepared in the same buffer as samples; all standards and samples were performed at least in duplicate. The Ab9 (human sequence Aβ1–16), 13.1.1 (end specific for Aβ40), and 2.1.3 (end specific for Aβ42) antibodies were used for two-site ELISA. Nunc MaxiSorp ELISA antibody coated plates (1 μg/well in PBS) were blocked with a solution of 2% Block Ace and 1% BSA in PBS overnight. Carboxyl-terminal (end-specific) antibodies were used for capture, to avoid an excess of one Aβ peptide from competing away the other, while HRP-conjugated Ab9 antibody was used as a detection antibody. The lower limit of detection was approximately 5 pM, with a linear range of about two orders of magnitude (~20–2000 pM). After development with TMB reagent, plates were stopped with 6% *o*-phosphoric acid and read at 450 nm using a BioTek multi-well plate reader.

Synaptosome preparation

Synaptosomes are often used in studies of the brain because they provide a complete model of a functional synapse composed of a continuous plasma membrane with functional pumps and channels capable of ion exchange, and responding to depolarization; therefore, they provide a reliable model of neuronal PtdSer asymmetry (Whittaker, 1993). Synaptosome fractions from 1, 6, 9, and 12 month-old APP/PS-1 human double knock-in mice were isolated as described previously (Bader Lange et al., 2008; Mohmmad Abdul and Butterfield, 2005) with modifications. Whole brain fractions were homogenized in an isolation buffer (0.32 M sucrose, 0.2 mM PMSF, 2 mM EDTA, 2 mM EGTA, 20 mM HEPES, 4 μg/ml leupeptin, 4 μg/ml pepstatin, 5 μg/ml aprotinin, and 20 μg/ml trypsin inhibitor). The homogenate was then centrifuged at 4000 rpm ($1940 \times g$) for 10 min at 0°C and supernatant decanted. The supernatant was centrifuged at 14,800 rpm ($25,400 \times g$) for 12 min at 0°C. The resulting pellet was mixed with a small volume of cold isolation buffer and layered onto cold discontinuous sucrose gradients containing 10 ml each of 1.18 M (pH 8.5), 1.0 M (pH 8.0), and 0.85 M (pH 8.0) sucrose, as well as 2 mM EDTA, 2 mM EGTA, and 10 mM HEPES. Gradients were centrifuged in a Beckman-Coulter Optima L-90K ultracentrifuge at 22,000 rpm ($82,500 \times g$) for 1 h at 4°C. Resulting purified synaptosomes were removed from the 1.18/1.0 M interface and washed three times in Locke's buffer (0.15 mM NaCl, 5.6 mM KCl, 2.3 mM $CaCl_2 \cdot 2\ H_2O$, 1.0 mM $MgCl_2 \cdot 6\ H_2O$, 3.6 mM $NaHCO_3$, 5.0 mM Glucose, and 5.0 mM HEPES; pH 7.4) at 15,500 rpm ($29,100 \times g$) for 12 min at 0°C. Protein concentrations were determined according to the Pierce BCA method (Pierce, Rockford, IL).

Annexin V Assay

This fluorescence assay was conducted as described previously (Castegna et al., 2004; Mohmmad Abdul and Butterfield, 2005) to directly study externalization of PtdSer. Synaptosomal samples (200μg) from each age-group were covered and incubated for 5 min in Annexin binding buffer (ABB) [10mM HEPES, 140mM NaCl, 2.5mM and $CaCl_2$; pH 7.4] and Annexin V FITC. Samples were then washed twice with ABB at 14,000 rpm ($23,700 \times g$) for 5 min at 4°C (Hettich Mikro 22 R microcentrifuge), and resuspended in 200μl ABB.

Residual fluorescence was measured in a Molecular Devices SpectraMAX Gemini fluorescence plate reader (wavelengths of Ex/Em: 494/518 nm). Exposed PtdSer is detected through its affinity for Annexin V (AV), a phospholipid binding protein coupled with a fluorescent tag, leading to increased fluorescence for samples in which the AV probe has bound exposed PtdSer.

NBD-PS assay

This assay was completed as previously described (Bader Lange et al., 2008; Comfurius et al., 1996) to indirectly study the externalization of PtdSer. Synaptosome samples from each age group (200 µg) were covered and incubated for 1 h with NBD-PS, then washed twice in Locke's buffer (pH 7.4) at 14,000 rpm ($23,700 \times g$) for 5 min at 4°C (Hettich Mikro 22 R microcentrifuge). After resuspension in 200 µl Locke's buffer (pH 7.4), samples were loaded onto a fluorescence plate and treated with 7.5 mM sodium dithionite ($Na_2S_2O_4$) to quench fluorescence by reduction of the exposed, NBD-labeled PtdSer (Fig. 1). Loss of residual fluorescence was measured in a Molecular Devices SpectraMAX Gemini fluorescence plate reader (wavelengths of Ex/Em: 460/514 nm).

This procedure leads to decreased fluorescence for samples in which the NBD-PS probe has integrated into the plasma membrane and reduction of the probe subsequently exposed onto the outer leaflet (Fig. 1); exposure of NBD-PS is a result of the loss of the cell's ability to maintain PtdSer asymmetry. The NBD-PS technique has a value-added characteristic of addressing potential concerns with AV-associated probe access to the inner leaflet of an unstable system, possibly creating an incorrect interpretation of asymmetric collapse (Castegna et al., 2004; Mohmmad Abdul and Butterfield, 2005). Another advantage of the NBD-PS assay is that highly ionic $Na_2S_2O_4$ does not readily diffuse through the bilayer.

Mg^{2+} ATPase activity assay

This assay was completed according to previous procedures (Castegna et al., 2004; Sadrzadeh et al., 1993) to indirectly analyze flippase activity. Synaptosomes (7.5 µg) from 1, 6, 9, and 12 month-old WT and APP/PS-1 mice were suspended in ATPase assay buffer (18 mM histidine, 18 mM imidazole, 80 mM NaCl, 15 mM KCl, 3mM $MgCl_2$, 0.1mM EGTA; pH 7.1) and treated with 0.1 mM of the Na^+K^+ ATPase inhibitor ouabain to a final volume of 100 µl in a microtiter plate. Plates were covered and incubated for 10 min at 37 °C, followed by addition of 3mM ATP, and a second 60 min incubation at 37 °C. After, 5 µl of 5% SDS was added to terminate the reaction and 125 µl of color reagent (0.36 g ascorbic acid mixed with 15 ml of molybdate acid solution) was added to each well. Mg^{2+} ATPase activity was measured with a BIO-TEK µ-Quant UV plate reader (810 nm) as the net amount of inorganic phosphate (P_i) produced by the enzyme after reaction with ATP (Sadrzadeh et al., 1993).

Caspase-3 1D-gel electophoresis and Western blotting

Total brain homogenate from 1, 6, 9, and 12 month-old WT and APP/PS-1 mice were separated by one-dimensional SDS-polyacrylamide gel electrophoresis (1D SDS-PAGE) using a Criterion precast 4–12% Bis-Tris gels and XT MES running buffer as previously described, with exceptions (Bader Lange et al., 2008). Samples (75 µg) were suspended in a Sample buffer (0.5 M Tris, pH 6.8; 40% glycerol, 8% SDS, 20% β-mercaptoethanol, and 0.01% bromophenol blue), then heated at 95 °C for 5 min prior to gel loading. Following separation by 1D-PAGE, proteins were transferred to nitrocellulose membranes using a Bio-RAD Trans-Blot Semi-dry Transfer Cell system at 20 V for 2 h. Membranes were blocked post-transfer with 3% bovine serum albumin (BSA) in wash blot (a PBS solution containing 0.04% (v/v) Tween 20 and 0.10 M NaCl) for 2 h at room temperature, then incubated with anti-rabbit polyclonal anti-caspase-3 (1:5000) and anti-mouse polyclonal anti-α-tubulin primary (1:8000) antibodies in Wash blot for 2 h at room temperature on a rocking platform. Blots were rinsed three times for 5 min each

in wash blot, then incubated with a 1:8000 dilution of anti-rabbit IgG and anti-mouse IgG HRP-linked secondary antibodies in wash blot for 1 h at room temperature on a rocking platform. Membranes were then rinsed three times for 10 min each in wash blot and developed using a 40:1 dilution of Amersham ECL-Plus Western blotting detection reagents A and B, respectively. Blots were scanned on a STORM Phosphoimager (440 nm) and quantified using the 1D-component of GE ImageQuant TL software (GE Healthcare, Pittsburgh, PA).

Statistics

All data are presented as mean ± S.E.M. and analyzed via GraphPad Prism 5.0 software for Windows (San Diego, CA). One-way ANOVA was used to determine the effect(s) of age on PtdSer asymmetry, Mg^{2+}ATPase activity, and caspase-3 levels in WT mice followed by a Tukey post-hoc analysis. Two-way ANOVA was used to determine the effect(s) of age and APP/PS-1 double knock-in genotype on PtdSer asymmetry, Mg^{2+}ATPase activity, and caspase-3 levels followed by a Bonferroni post-hoc analysis; $P<0.05$ was considered to be significantly different.

Results

SDS-Soluble Aβ(1–40) and Aβ(1–42) levels as a function of age in APP/PS-1 mouse brain

SDS-soluble Aβ(1–40) and Aβ(1–42) levels in brain from 1, 3, 6, 9, and 12 month-old APP/PS-1 mice were quantified using a two-site sandwich ELISA. This procedure is widely utilized to extract and quantitate levels of soluble Aβ(1–40) and Aβ(1–42) (Das et al., 2003; Kukar et al., 2005; McGowan et al., 2005; Murphy et al., 2007). Moreover, these APP/PS-1 mice are known to have significantly more Aβ(1–40) and Aβ(1–42) than WT mice at all ages (Anantharaman et al., 2006; Murphy et al., 2007; Reaume et al., 1996; Siman et al., 2000). Although masked by y-axis scaling, the current results do demonstrate the presence of SDS-soluble Aβ(1–42) as early as 1 month of age (Fig. 2b), and a significant age-dependent increase in SDS-soluble Aβ(1–40) and Aβ(1–42) levels (Fig. 2 a & b).

Brains from 1 month-old APP/PS-1 mice were used as the control from which to compare the SDS-soluble Aβ load in 3, 6, 9, and 12 month-old APP/PS-1 mice. The age-related increase in Aβ(1–40) and Aβ(1–42) levels begins at 3 months of age, although not significant, [Fig. 2 a & b], and continues to rise 500-fold in Aβ(1–40) and 300-fold in Aβ(1–42) at 12 months of age relative to 1 month-old mice [Fig. 2a, Aβ(1–40), ***$P<0.001$; Fig. 2b, Aβ(1–42), ***$P<0.001$]. Moreover, the levels of Aβ(1–40) are slightly higher than Aβ(1–42) at all ages, consistent with the fact that Aβ(1–40) is produced in greater abundance (Burdick et al., 1992; Jarrett et al., 1993).

FA-Soluble Aβ(1–40) and Aβ(1–42) levels as a function of age in APP/PS-1 mouse brain

FA-soluble Aβ(1–40) and Aβ(1–42) levels in brain from 1, 3, 6, 9, and 12 month-old *APP/PS-1* mice were quantified using two-site sandwich ELISA, in order to extract and quantitate levels of insoluble Aβ(1–40) and Aβ(1–42), a typical component of neuritic plaques (Das et al., 2003; Kukar et al., 2005; McGowan et al., 2005; Murphy et al., 2007). The results demonstrate an age-dependent increase in FA-soluble Aβ(1–40) and Aβ(1–42) [Fig. 3 a & b] compared to 1 month-old APP/PS-1 control mice. FA-soluble Aβ(1–42) levels begin increasing at 3 months-old (Fig. 3b), though not significantly, and continue to rise significantly 100-fold at 12 months of age (Fig. 3b, **$P<0.01$). FA-soluble Aβ(1–40) levels, however, do not begin an age-dependent trend until 6 months-old (Fig. 3a). Most notably, the amount of FA-soluble Aβ(1–42) is at all ages greater than that of Aβ(1–40), as Aβ(1–42) is known to be considerably more prone to and faster at oligomerization and subsequent fibril formation than the more abundantly produced Aβ(1–40) (Burdick et al., 1992; Jarrett et al., 1993).

Annexin V fluorescence in synaptosomes from brain of wild-type and APP/PS-1 mice

To assess the effects of normal aging on exposure of PtdSer to the outer-leaflet of the lipid bilayer, synaptosomes extracted from whole brain of 1 month-old WT mice were used as a control to compare synaptosomes isolated from whole brain of 6, 9, and 12 month-old WT mice. The results demonstrate a significant increase in AV fluorescence beginning at 6 months-old (Fig. 4a, *P<0.05), an increase that remains significant at 9 and 12 months (Fig. 4a, 9 months-old, ***P<0.001; 12 months-old, **P<0.01). These results are consistent with the well-known increase in brain oxidative stress with age (Butterfield and Stadtman, 1997) that can lead to cell death.

In order to assess trends in age-related effects of brain aging in WT mice and this knock-in mouse model of Aβ pathology as indexed by AV-detected PtdSer exposure, AV-associated fluorescence in synaptosomes of 1, 6, 9, and 12 month-old APP/PS-1 mice was analyzed relative to that of 1 month-old WT mice as a control (Fig. 4b). AV fluorescence is significantly increased at 9 and 12 months of age in brain of APP/PS-1 mice compared to 1 month-old WT control mice (Fig. 4b, 9 months-old, ***P<0.001; 12 months-old, ***P<0.001). Moreover, there was a significant increase in 9 and 12 month-old APP/PS-1 AV fluorescence compared to their respective 9 and 12 month, age-matched WT mice (Fig. 4b, 9 month-old, **P<0.01; 12 month-old, ***P<0.001), demonstrating that the APP/PS-1 genotype affects PtdSer exposure significantly more than normal aging alone. Interestingly, both WT and APP/PS-1 mice exhibit an age-related increase in AV fluorescence from 6 to 9 months-old (Fig. 4a, *P<0.05; Fig. 4b, ***P<0.001). However, this fluorescence increase was significantly more prominent in APP/PS-1 mice, which directly correlates with significant Aβ(1–42) deposition reported to begin at 9 months of age in this FAD mouse model (Anantharaman et al., 2006;Reaume et al., 1996;Siman et al., 2000).

NBD-PS fluorescence in synaptosomes from brain of wild-type and APP/PS-1 mice

A second method was used to examine the effect of age on PtdSer asymmetry in synaptosomes prepared from 1, 6, 9, and 12 month-old WT and APP/PS-1 mice. As indicated in Fig. 1, loss of NBD-PS fluorescence is observed if PtdSer is exposed onto the outer bilayer leaflet. In order to avoid graphical results showing negative values (with consequent downward-facing bar graphs), data were analyzed as a percentage of control values set to 100%, yielding a graphical presentation more familiar to biochemical assays. As with AV studies, the effects of normal aging on exposure of PtdSer was assessed by comparing synaptosomes extracted from whole brain of 1 month-old control WT mice to synaptosomes isolated from 6, 9, and 12 month-old WT mice. The results show a significant decrease in NBD-PS fluorescence beginning at 9 months (Fig. 5a, ***P<0.001) that remains significant to 12 months-old (Fig. 5a, ***P<0.001); again, consistent with the well-known increase in brain oxidative stress with age (Butterfield and Stadtman, 1997), which leads to neuronal cell death.

To assess trends in age-related brain aging in WT and APP/PS-1 mice, NBD-PS fluorescence in synaptosomes isolated from brain of 1, 6, 9, and 12 month-old APP/PS-1 mice was analyzed relative to that of 1 month-old WT mice as a control (Fig. 5b). NBD-PS fluorescence is significantly lost at 9 and 12 months-old in brain from APP/PS-1 mice compared to 1month-old WT control brain (Fig. 5b, 9 months-old, ***P<0.001; 12 months-old, ***P<0.001). Moreover, there was a significant decrease in 12 month-old APP/PS-1 fluorescence compared to age-matched, 12 month-old WT mice (Fig. 5b, **P<0.01), illustrating once again that the APP/PS-1 genotype has a significantly greater affect on PtdSer outer-leaflet exposure than normal aging alone.

Also consistent with the AV-assessed loss of PtdSer asymmetry noted above, both WT and APP/PS-1 mice exhibit a significant age-related decrease in NBD-PS fluorescence from 6 to

9 months of age (Fig. 5 a & b, ***P<0.001), which is more prominent in APP/PS-1 mice and correlates with significant Aβ(1–42) deposition in this FAD model (Anantharaman et al., 2006; Reaume et al., 1996; Siman et al., 2000). Interestingly, however, there is significantly greater maintenance of PtdSer asymmetry in brain from 1 and 6 month-old APP/PS-1 mice compared to 1 month-old WT controls (Fig. 5b, 1 month-old, †††P<0.001; 6 months-old, †P<0.05), in agreement with the notion that the APP/PS-1 mouse brain responds to elevated oxidative stress associated with Aβ(1–42) at an early age (Abdul et al., 2008).

Mg^{2+}ATPase activity in synaptosomes from brain of wild-type and APP/PS-1 mice

Determination of Mg^{2+}ATPase activity was utilized to indirectly represent the activity of the ATP-dependent, membrane-bound translocase, flippase, as highly specific antibodies to flippase have not yet been obtained (Auland et al., 1994). The effect of normal aging on Mg^{2+}ATPase activity was assessed by comparison of 6, 9, and 12 month-old synaptosomes to that of 1 month-old WT mice as a control. The results demonstrate a significant age-related decrease in enzyme activity beginning at 9 months-old (Fig. 6a, *P<0.05), a decrease that becomes even more significant at 12 months of age (Fig. 6a, **P<0.01). As with AV and NBD-PS fluorescence above, these results are also congruent with previous reports of increasing oxidative stress in brain due to normal aging processes (Butterfield and Stadtman, 1997).

The age-related effect of brain aging in WT and APP/PS-1 mice on Mg^{2+}ATPase activity was assessed by comparison of synaptosomes of 1, 6, 9, and 12 month-old WT and APP/PS-1 mice to 1 month-old WT mice as a control (Fig. 6b). Like WT aging trends, APP/PS-1 mice show a significant decrease in Mg^{2+}ATPase activity starting at 9 months-old (Fig. 6a, **P<0.01) that becomes even more significant at 12 months (Fig. 6b, ***P<0.001) compared to 1 month-old WT controls. Moreover, at 12 months-old, there was a significant decrease in enzyme activity in APP/PS-1 mice compared to 12 month, age-matched WT mice (Fig. 6b, ***P<0.001), illustrating that the APP/PS-1 double knock-in genotype significantly affects the activity of all Mg^{2+}ATPase enzymes, including flippase, to a greater extent than simply aging alone.

Interestingly, APP/PS-1 mice exhibit a significant age-related decrease in enzyme activity from 6 to 9 months (Fig. 6b, ***P<0.001) that directly correlates with significant Aβ(1–42) deposition reported to begin at 9 months-old in this FAD mouse model (Anantharaman et al., 2006;Reaume et al., 1996;Siman et al., 2000). However, it worth noting that this trend is contrasted by either greater maintenance or expression of Mg^{2+}ATPases in the plasma membrane from 1 to 6 months-old in APP/PS-1 mice (Fig. 6b, †P<0.05), that is also significant between 6 month-old WT and age-matched APP/PS-1 mice (Fig. 6b, †††P<0.001). Consistent with both AV and NBD-PS data, this particular trend is congruent with the idea that young APP/PS-1 mouse brain elicits a significant, potentially protective, response to elevated oxidative stress associated with Aβ(1–42) (Abdul et al., 2008).

Caspase-3 Levels in brain of wild-type and APP/PS-1 mice

Pro-apoptotic caspase-3 is synthesized as a cytosolic, inactive precursor (36 kDa), that is cleaved into two active fragments of 20 kDa (p18; amino acids 29–175) and 18 kDa (p12; amino acids 176–277), upon activation by apoptotic stimuli. The anti-caspase-3 primary antibody used was chosen for its ability to recognize and probe all three forms of caspase-3 on Western blots, while α-tubulin was used to normalize. In order to examine the effect of normal aging on levels and activation of procasepase-3 and its two active fragments, whole brain homogenate of 6, 9, and 12 month-old WT mice was blotted and analyzed with respect to 1 month-old WT mice as a control (Fig. 7, 8, & 9). Interestingly, procaspase-3 levels steadily decrease with age (Fig. 7 a & b), becoming significant at 12 months-old (Fig. 7b, *P<0.05). This age-associated decrease in procaspase-3 levels with age is mirrored in brain 1, 6, 9, and

12 month-old APP/PS-1 mice compared to 1 month-old WT controls, ostensibly emulating trends in NBD-PS fluorescence, in that, there is a large increase in procaspase-3 levels in APP/PS-1 brain at 6 months of age, although not significant, followed by steadily decreasing procaspase-3 levels with age (Fig. 7 a & c).

In contrast to procaspase-3, analysis of the levels of the p18, 20 kDa active fragment of caspase-3 in 6, 9, and 12 month-old WT mice compared to 1 month-old WT controls shows a tendency to increase with age, becoming significant at 9 months-old (Fig. 8 a & b, **$P<0.01$). This trend is also reflected in brain of 1, 6, 9, and 12 month-old APP/PS-1 mice compared to 1 month-old WT animals, with a significant increase in p18 appearing at 9 months-old (Fig. 8 a & c, ***$P<0.001$) and continuing through 12 months of age (Fig. 8 a & c, ***$P<0.001$). In addition, there was a significant increase in both 9 and 12 month-old APP/PS-1 p18 levels compared to respective age-matched, 9 and 12 month WT brain (Fig. 8c, 9 & 12 months-old, *$P<0.05$), suggesting the APP/PS-1 knock-in genotype causes significantly more apoptosis in aging mouse brain than normal aging alone. Finally, the significant increase in p18 levels from 6 to 9 months in brain of APP/PS-1 mice (Fig. 8c, *$P<0.05$) correlates with significant Aβ(1–42) deposition reported to begin at 9 months in this mutant mouse model (Anantharaman et al., 2006; Reaume et al., 1996; Siman et al., 2000).

Interestingly, the 18 kDa, p12 active fragment of caspase-3 follows a remarkably different trend altogether, in that there does not appear to be an age-associated increase or decrease in levels of this particular active fragment in either WT or APP/PS-1 mice (Fig. 9). Instead, both WT and APP/PS-1 mice demonstrate a significant increase in p12 levels at 9 months of age (Fig. 9b, **$P<0.01$; Fig. 9c, *$P<0.05$) compared to 1 month-old WT controls that disappears as mice age from 9 to 12 months (Fig. 9 b & c). However, it should be noted that these results do show a significant increase in pro-apoptotic p12 at the age when significant Aβ(1–42) deposition is reported to occur in brain of this FAD mouse model (Anantharaman et al., 2006; Reaume et al., 1996; Siman et al., 2000).

Discussion

Analysis of synaptosomes from age-matched WT and APP/PS-1 mice by AV and NBD-PS assay confirms the hypothesis that PtdSer asymmetry is significantly altered in brain of this FAD mouse model beginning at 9 months, in parallel with significant Aβ(1–42) deposition and oxidative stress (Anantharaman et al., 2006; Mohmmad Abdul et al., 2006; Mohmmad Abdul et al., 2008; Reaume et al., 1996; Siman et al., 2000). Both WT and APP/PS-1 mice follow a similar trend in PtdSer exposure with age, which suggests a significant collapse in PtdSer asymmetry as a function of age (Fig. 4 & 5). However, the fundamental difference between the loss of lipid asymmetry found in WT mice and that of APP/PS-1 mice is the trend from 6 to 12 months of age. The age-related increase in AV and decrease in NBD-PS fluorescence from 6 to 12 months-old is greater in APP/PS-1 mice than WT mice (Fig. 4 & 5), demonstrating that even though outer leaflet exposure of PtdSer becomes increasingly apparent in aging mice, the degree of exposure is augmented in APP/PS-1 brain.

Furthermore, the present AV, NBD-PS, and ELISA results illustrate that significant PtdSer exposure corresponds to the age at which significant Aβ deposition occurs (9 months, Fig. 2, 4, & 5), and not of plaque deposition (12 months, Fig. 3, 4, & 5). This finding, along with previous studies of Aβ levels in APP/PS-1 mice (Anantharaman et al., 2006; Mohmmad Abdul et al., 2006; Murphy et al., 2007; Siman et al., 2000), suggests that elevated levels of SDS-soluble, oligomeric Aβ species, in addition to increased oxidative stress (Butterfield et al., 2002; Butterfield and Lauderback, 2002; 2007; LaFontaine et al., 2002; Mohmmad Abdul et al., 2008), in APP/PS-1 brain may contribute to altered PtdSer plasma membrane localization beyond the effects of normal brain aging.

The significant rise in NBD-PS fluorescence in 1 and 6 month-old APP/PS-1 brain compared to 1 month WT controls (Fig. 5) implies that PtdSer externalization is an important dynamic in the ongoing neurodegeneration found in FAD brain, prior to significant Aβ or plaque deposition, potentially representing a stage of toxic Aβ(1–42) oligomer formation. APP/PS-1 mice have been shown to have accumulated Aβ as early as 1 day old (Mohmmad Abdul et al., 2006), and present ELISA results demonstrate a visible increase in SDS-soluble Aβ(1–42) from 1 to 3 months-old that continues to escalate significantly with age (Fig. 2b) in parallel to increasing oxidative stress levels previously measured in this same APP/PS-1 double knock-in mouse (Mohmmad Abdul et al., 2008). Studies in 6 month-old Tg2576 mice expressing APP mutations similar to this study (Hsiao et al., 1996) reveal that neuropathological changes and memory impairment occur long before Aβ plaque deposition, correlating with levels of various soluble Aβ oligomers (Hsia et al., 1999;Lesne et al., 2006;Mucke et al., 2000;Westerman et al., 2002).At these young ages, it is reasonable to speculate that APP/PS-1 brain has up-regulated various neuroprotective systems, not yet overcome by oxidative stress conditions induced, in part, by toxic Aβ(1–42). Up-regulation of a cellular stress response is a well-known course of action employed by neuronal cells to combat damage (Calabrese et al., 2007;Poon et al., 2004), and could explain the enrichment of PtdSer to the inner leaflet of the lipid bilayer from 1 to 6 months-old.

Upon initiating a stress response, cells commonly up-regulate antioxidants and various proteins involved in maintenance of PtdSer asymmetry, including the enzyme flippase, represented by increasing Mg^{2+}ATPase activity at 6 months of age (Fig. 6). The ATP-dependent translocase flippase is an integral membrane protein that actively maintains the asymmetrical distribution of PtdSer onto the inner-leaflet of the bilayer (Daleke and Lyles, 2000;Daleke, 2003;Paulusma and Oude Elferink, 2005). During both WT and APP/PS-1 mouse aging, oxidative stress intensifies beyond the capacity of the stress response (Mohmmad Abdul et al., 2008), damaging this enzyme, and resulting in the age-dependent collapse of PtdSer asymmetry, from 6 to 12 months of age (Fig. 4,5,& 6). Flippase activity is dependent on a critical cysteine residue within its primary structure (Daleke and Lyles, 2000;Daleke, 2003;Paulusma and Oude Elferink, 2005). Oxidative stress induces production of reactive alkenals, HNE and acrolein, within the bilayer that diffuse rapidly from their formation sites (Butterfield and Stadtman, 1997;Butterfield et al., 2006;Lovell et al., 2001;Markesbery and Lovell, 1998). HNE and acrolein are known to form Michael adducts with cysteine residues, which would inhibit flippase activity (Castegna et al., 2004;Daleke and Lyles, 2000;Daleke, 2003;Mohmmad Abdul et al., 2008;Paulusma and Oude Elferink, 2005;Tyurina et al., 2004).

Like HNE and acrolein, Aβ(1–42) oligomers continually form throughout FAD progression and can initiate lipid peroxidation events (Butterfield et al., 2002; Butterfield, 2002; Butterfield and Lauderback, 2002; 2007; Schubert et al., 1995), either by membrane penetration or surface binding. Each Aβ-bilayer interaction is possible since Aβ(1–42) peptides are both hydrophobic and inherently attracted to negatively charged phospholipid head-groups, such as PtdSer (McLaurin and Chakrabartty, 1997). Depending on the avenue of association, oligomers can have a Ca^{2+} mobilizing effect through direct interaction with membrane receptors (Demuro et al., 2005; Snyder et al., 2005), destabilize membrane structure by increasing its permeability and fluidity (Demuro et al., 2005; Kayed et al., 2004; Muller et al., 1995; Sokolov et al., 2006), and induce oxidative stress leading to dysregulation of mitochondria (Butterfield et al., 2002; Butterfield, 2002; Butterfield and Lauderback, 2002; 2007; Drake et al., 2003; Lambert et al., 1998; Mattson, 2004; Schubert et al., 1995). Thus, by 9 months-old, extensive oxidative stress, in tandem with mounting Aβ(1–42) production with age in brains of APP/PS-1 mice, could be significant enough to overwhelm initial neuroprotective stress responses and significantly cause loss of PtdSer membrane asymmetry beyond that of the normal aged brain (Fig. 2, 4, 5, & 6).

Ca^{2+} mobilization, whether Aβ(1–42)- and/or alkenal-induced, is noteworthy since flippase is known to be sensitive towards alterations in Ca^{2+} homeostasis (Castegna et al., 2004; Mohmmad Abdul and Butterfield, 2005). An influx of 0.2 µM or higher $[Ca^{2+}]_i$ can significantly affect the translocating ability of flippase (Bitbol et al., 1987; Daleke, 2003). Prior studies using *in vitro* and *in vivo* systems, however, suggest Ca^{2+} dysregulation is not the main contributor to asymmetric collapse, but rather, a secondary effect of oxidation events or other membrane alterations that lead to detrimental Ca^{2+} influx (Castegna et al., 2004; Mohmmad Abdul and Butterfield, 2005). For that reason, plasma membrane structural integrity should be considered important.

Stability of the plasma membrane is generally associated with cholesterol, whose rigid structure allows it to integrate between phospholipid head-groups and modulate membrane fluidity. Previous studies with APP/PS-1 mice reveal declining membrane cholesterol levels correlate inversely with brain Aβ(1–42) levels (George et al., 2004; Wirths et al., 2006). Enriching PC12 cells with exogenous cholesterol (i.e. reducing fluidity) makes them resistant to the cytotoxic action of soluble Aβ peptides, while reducing membrane cholesterol (i.e. increasing fluidity) made cells more vulnerable (Arispe and Doh, 2002). Furthermore, cholesterol depletion can stimulate an increase in lipid peroxidation (Lopez-Revuelta et al., 2005), resulting in significant PtdSer externalization by decreased flippase activity (Lopez-Revuelta et al., 2007). Taken as a whole, this research suggests increased membrane fluidity would provide oligomers the opportunity to adversely affect PtdSer leaflet distribution and integral membrane protein (e.g. flippase) function.

The age-related loss of synaptosomal PtdSer asymmetry of APP/PS-1 mice is remarkable in other ways as well. Exposure of PtdSer to the outer membrane leaflet is a well-known signal for phagocytosis and can denote the initial stages of apoptosis (Fadok et al., 1992; Kagan et al., 2003; Paulusma and Oude Elferink, 2005; Tyurina et al., 2004). Most notably, PtdSer externalization is found downstream of caspase-3 activation under oxidative stress conditions (Mandal et al., 2002; Martin et al., 1996; Nicholson, 1999; Vanags et al., 1996). In studies of non-neuronal, red blood cells, caspase-3 activation is also associated with loss of flippase translocase activity (Mandal et al., 2005). Results of the current study confirm that apoptosis is an ongoing process in APP/PS-1 mouse brain as early as 1 month-old, as indicated by the presence of p18 (20 kDa) and p12 (18 kDa) active fragments of caspase-3 (Fig. 8 & 9), which are reported to be found only in cells undergoing apoptosis (Nicholson et al., 1995). Furthermore, the increasing levels of both p18 and p12 fragments beginning at 9 months is also congruent with AV, NBD-PS, and Mg^{2+}ATPase data, which all show significant changes occurring between the ages of 6 and 9 months-old, emphasizing the importance of this time point in disease progression in brain of this mouse model of FAD. Interestingly, however, procaspase-3 levels steadily decrease with WT and APP/PS-1 animal age, though more significantly in APP/PS-1 brain (Fig. 7). Considering there is a steady increase in oxidative stress and Aβ(1–42) pathology in APP/PS-1 mouse brain, as well as a gradual increase in active caspase-3 fragment levels, it is reasonable to believe that the observed inverse relationship is due to increased activation and cleavage of procaspase-3 into p18 and p12 active fragments with disease progression.

The current results are consistent with the notion that PtdSer indicates not only mounting oxidative stress and Aβ pathology in FAD, but also apoptosis at its earliest stages. Supporting this notion, we observed loss of PtdSer asymmetry in brain from subjects with AD and, arguably its earliest form, amnestic MCI, that was associated with induction of caspase-3 levels (Bader Lange et al., 2008), while another study reported a significant increase in oxidative stress beginning at 1 month-old in this same APP/PS-1 double knock-in FAD mouse model (Mohmmad Abdul et al., 2008). Significant inner-leaflet enrichment of PtdSer at 1 and 6 months-old perhaps signifies an already well-advanced cell stress response, while the

diminution of inner-leaflet PtdSer levels from 6 to 9 months suggests the elicited stress response was effectively overcome by harsh conditions generated during disease progression in this FAD mouse model.

Conceivably, phospholipase A2, known to be altered in AD (Moses et al., 2006; Chalbot et al., 2009), could contribute to exposure of PtdSer to the external leaflet in synaptosomes from APP/PS-1 mice. However, PLA2 from snake venom does not lead to significant exposure of PtdSer in synaptosomal membranes (Ghassemi and Rosenberg, 1992). Hence, though PLA2 may play a role in what we observed in this study, the likelihood of such a role is small.

In summary, this study represents the first age-dependent investigation of PtdSer asymmetry in a mouse model of FAD by addressing how loss of PtdSer asymmetry may relate to pro-apoptotic factor expression and toxic Aβ(1–42) accumulation.

Acknowledgments

References

Abdul HM, Sultana R, St Clair DK, Markesbery WR, Butterfield DA. Oxidative damage in brain from human mutant APP/PS-1 double knock-in mice as a function of age. Free Radic. Biol. Med 2008;45:1420–1425. [PubMed: 18762245]

Anantharaman M, Tangpong J, Keller JN, Murphy MP, Markesbery WR, Kiningham KK, St Clair DK. β-Amyloid mediated nitration of manganese superoxide dismutase: Implication for oxidative stress in a APP$^{NLH/NLH}$ X PS-1$^{P264L/P264L}$ double knock-in mouse model of Alzheimer's disease. Am. J. Pathol 2006;168:1608–1618. [PubMed: 16651627]

Arispe N, Doh M. Plasma membrane cholesterol controls the cytotoxicity of Alzheimer's disease AβP (1–40) and (1–42) peptides. FASEB J 2002;16:1526–1536. [PubMed: 12374775]

Auland ME, Roufogalis BD, Devaux PF, Zachowski A. Reconstitution of ATP-dependent aminophospholipid translocation in proteoliposomes. Proc. Natl. Acad. Sci. U.S.A 1994;91:10938–10942. [PubMed: 7971987]

Bader Lange ML, Cenini G, Piroddi M, Abdul HM, Sultana R, Galli F, Memo M, Butterfield DA. Loss of phospholipid asymmetry and elevated brain apoptotic protein levels in subjects with amnestic mild cognitive impairment and Alzheimer disease. Neurobiol. Dis 2008;29:456–464. [PubMed: 18077176]

Berman DE, Dall'Armi C, Voronov SV, McIntire LB, Zhang H, Moore AZ, Staniszewski A, Arancio O, Kim TW, Di Paolo G. Oligomeric amyloid-β peptide disrupts phosphatidylinositol-4,5-bisphosphate metabolism. Nat. Neurosci 2008;11:547–554. [PubMed: 18391946]

Bitbol M, Fellmann P, Zachowski A, Devaux PF. Ion regulation of phosphatidylserine and phosphatidylethanolamine outside-inside translocation in human erythrocytes. Biochim. Biophys. Acta 1987;904:268–282. [PubMed: 3117114]

Borchelt DR, Ratovitski T, van Lare J, Lee MK, Gonzales V, Jenkins NA, Copeland NG, Price DL, Sisodia SS. Accelerated amyloid deposition in the brains of transgenic mice coexpressing mutant presenilin-1 and amyloid precursor proteins. Neuron 1997;19:939–945. [PubMed: 9354339]

Burdick D, Soreghan B, Kwon M, Kosmoski J, Knauer M, Henschen A, Yates J, Cotman C, Glabe C. Assembly and aggregation properties of synthetic Alzheimer's A4/β amyloid peptide analogs. J. Biol. Chem 1992;267:546–554. [PubMed: 1730616]

Butterfield DA, Stadtman ER. Protein oxidation processes in aging brain. Adv. Cell Aging Gerontol 1997;2:161–191.

Butterfield DA, Castegna A, Lauderback CM, Drake J. Evidence that amyloid β-peptide-induced lipid peroxidation and its sequelae in Alzheimer's disease brain contribute to neuronal death. Neurobiol. Aging 2002;23:655–664. [PubMed: 12392766]

Butterfield DA. Amyloid β-peptide (1–42)-induced oxidative stress and neurotoxicity: Implications for neurodegeneration in Alzheimer's disease brain. A review. Free Radic. Res 2002;36:1307–1313. [PubMed: 12607822]

Butterfield DA, Lauderback CM. Lipid peroxidation and protein oxidation in Alzheimer's disease brain: Potential causes and consequences involving amyloid β-peptide-associated free radical oxidative stress. Free Radic. Biol. Med 2002;32:1050–1060. [PubMed: 12031889]

Butterfield DA, Reed T, Perluigi M, De Marco C, Coccia R, Cini C, Sultana R. Elevated protein-bound levels of the lipid peroxidation product, 4-hydroxy-2-nonenal, in brain from persons with mild cognitive impairment. Neurosci. Lett 2006;397:170–173. [PubMed: 16413966]

Butterfield DA, Reed T, Newman SF, Sultana R. Roles of amyloid β-peptide-associated oxidative stress and brain protein modifications in the pathogenesis of Alzheimer's disease and mild cognitive impairment. Free Radic. Biol. Med 2007;43:658–677. [PubMed: 17664130]

Cai XD, Golde TE, Younkin SG. Release of excess amyloid-β protein from a mutant amyloid-β protein precursor. Science 1993;259:514–516. [PubMed: 8424174]

Calabrese V, Mancuso C, Sapienza M, Puleo E, Calafato S, Cornelius C, Mangiameli A, Di Mauro M, Stella AM, Castellino P. Oxidative stress and cellular stress response in diabetic nephropathy. Cell Stress Chaperones 2007;12:299–306. [PubMed: 18229449]

Castegna A, Lauderback CM, Mohmmad-Abdul H, Butterfield DA. Modulation of phospholipid asymmetry in synaptosomal membranes by the lipid peroxidation products, 4-hydroxynonenal and acrolein: Implications for Alzheimer's disease. Brain Res 2004;1004:193–197. [PubMed: 15033435]

Chalbot S, Zetterberg H, Blennow K, Bladby T, Grundke-Iqbal I, Iqbal K. Cerebrospinal fluid secretory Ca^{2+}-dependent phospholipase A2 activity is increased in Alzheimer disease. Clin. Chem 2009;55:2171–2179. [PubMed: 19850632]

Citron M, Oltersdorf T, Haass C, McConlogue L, Hung AY, Seubert P, Vigo-Pelfrey C, Lieberburg I, Selkoe DJ. Mutation of the β-amyloid precursor protein in familial Alzheimer's disease increases β-protein production. Nature 1992;360:672–674. [PubMed: 1465129]

Comfurius P, Williamson P, Smeets EF, Schlegel RA, Bevers EM, Zwaal RF. Reconstitution of phospholipid scramblase activity from human blood platelets. Biochemistry 1996;35:7631–7634. [PubMed: 8672463]

Daleke DL, Lyles JV. Identification and purification of aminophospholipid flippases. Biochim. Biophys. Acta 2000;1486:108–127. [PubMed: 10856717]

Daleke DL. Regulation of transbilayer plasma membrane phospholipid asymmetry. J. Lipid Res 2003;44:233–242. [PubMed: 12576505]

Das P, Howard V, Loosbrock N, Dickson D, Murphy MP, Golde TE. Amyloid-β immunization effectively reduces amyloid deposition in *FcRγ*−/− knock-out mice. J. Neurosci 2003;23:8532–8538. [PubMed: 13679422]

Demuro A, Mina E, Kayed R, Milton SC, Parker I, Glabe CG. Calcium dysregulation and membrane disruption as a ubiquitous neurotoxic mechanism of soluble amyloid oligomers. J. Biol. Chem 2005;280:17294–17300. [PubMed: 15722360]

Drake J, Link CD, Butterfield DA. Oxidative stress precedes fibrillar deposition of Alzheimer's disease amyloid β-peptide (1–42) in a transgenic *Caenorhabditis elegans* model. Neurobiol. Aging 2003;24:415–420. [PubMed: 12600717]

Fadok VA, Voelker DR, Campbell PA, Cohen JJ, Bratton DL, Henson PM. Exposure of phosphatidylserine on the surface of apoptotic lymphocytes triggers specific recognition and removal by macrophages. J. Immunol 1992;148:2207–2216. [PubMed: 1545126]

George AJ, Holsinger RM, McLean CA, Laughton KM, Beyreuther K, Evin G, Masters CL. APP intracellular domain is increased and soluble Aβ is reduced with diet-induced hypercholesterolemia in a transgenic mouse model of Alzheimer disease. Neurobiol. Dis 2004;16:124–132. [PubMed: 15207269]

Ghassemi A, Rosenberg P. Effects of snake venom phospholipase A2 toxins (beta-bungarotoxin, notexin) and enzymes (Naja naja atra, Naja nigricollis) on aminophospholipid asymmetry in rat cerebrocortical synaptosomes. Biochem. Pharmacol 1992;44:1073–1083. [PubMed: 1417932]

Hertel C, Terzi E, Hauser N, Jakob-Rotne R, Seelig J, Kemp JA. Inhibition of the electrostatic interaction between β-amyloid peptide and membranes prevents β-amyloid-induced toxicity. Proc. Natl. Acad. Sci. U. S. A 1997;94:9412–9416. [PubMed: 9256496]

Hsia AY, Masliah E, McConlogue L, Yu GQ, Tatsuno G, Hu K, Kholodenko D, Malenka RC, Nicoll RA, Mucke L. Plaque-independent disruption of neural circuits in Alzheimer's disease mouse models. Proc. Natl. Acad. Sci. U. S. A 1999;96:3228–3233. [PubMed: 10077666]

Hsiao K, Chapman P, Nilsen S, Eckman C, Harigaya Y, Younkin S, Yang F, Cole G. Correlative memory deficits, Aβ elevation, and amyloid plaques in transgenic mice. Science 1996;274:99–102. [PubMed: 8810256]

Jarrett JT, Berger EP, Lansbury PT Jr. The carboxy terminus of the β amyloid protein is critical for the seeding of amyloid formation: Implications for the pathogenesis of Alzheimer's disease. Biochemistry 1993;32:4693–4697. [PubMed: 8490014]

Johansson AS, Garlind A, Berglind-Dehlin F, Karlsson G, Edwards K, Gellerfors P, Ekholm-Pettersson F, Palmblad J, Lannfelt L. Docosahexaenoic acid stabilizes soluble amyloid-β protofibrils and sustains amyloid-β-induced neurotoxicity *in vitro*. FEBS J 2007;274:990–1000. [PubMed: 17227385]

Kagan VE, Borisenko GG, Serinkan BF, Tyurina YY, Tyurin VA, Jiang J, Liu SX, Shvedova AA, Fabisiak JP, Uthaisang W, Fadeel B. Appetizing rancidity of apoptotic cells for macrophages: Oxidation, externalization, and recognition of phosphatidylserine. Am. J. Physiol. Lung Cell. Mol. Physiol 2003;285:L1–L17. [PubMed: 12788785]

Kayed R, Sokolov Y, Edmonds B, McIntire TM, Milton SC, Hall JE, Glabe CG. Permeabilization of lipid bilayers is a common conformation-dependent activity of soluble amyloid oligomers in protein misfolding diseases. J. Biol. Chem 2004;279:46363–46366. [PubMed: 15385542]

Kukar T, Murphy MP, Eriksen JL, Sagi SA, Weggen S, Smith TE, Ladd T, Khan MA, Kache R, Beard J, Dodson M, Merit S, Ozols VV, Anastasiadis PZ, Das P, Fauq A, Koo EH, Golde TE. Diverse compounds mimic Alzheimer disease-causing mutations by augmenting Aβ42 production. Nat. Med 2005;11:545–550. [PubMed: 15834426]

LaFontaine MA, Mattson MP, Butterfield DA. Oxidative stress in synaptosomal proteins from mutant presenilin-1 knock-in mice: Implications for familial Alzheimer's disease. Neurochem. Res 2002;27:417–421. [PubMed: 12064358]

Lambert MP, Barlow AK, Chromy BA, Edwards C, Freed R, Liosatos M, Morgan TE, Rozovsky I, Trommer B, Viola KL, Wals P, Zhang C, Finch CE, Krafft GA, Klein WL. Diffusible, nonfibrillar ligands derived from Aβ(1–42) are potent central nervous system neurotoxins. Proc. Natl. Acad. Sci. U. S. A 1998;95:6448–6453. [PubMed: 9600986]

Lauderback CM, Hackett JM, Huang FF, Keller JN, Szweda LI, Markesbery WR, Butterfield DA. The glial glutamate transporter, GLT-1, is oxidatively modified by 4-hydroxy-2-nonenal in the Alzheimer's disease brain: The role of Aβ(1–42). J. Neurochem 2001;78:413–416. [PubMed: 11461977]

Lesne S, Koh MT, Kotilinek L, Kayed R, Glabe CG, Yang A, Gallagher M, Ashe KH. A specific amyloid-β protein assembly in the brain impairs memory. Nature 2006;440:352–357. [PubMed: 16541076]

Lopez-Revuelta A, Sanchez-Gallego JI, Hernandez-Hernandez A, Sanchez-Yague J, Llanillo M. Increase in vulnerability to oxidative damage in cholesterol-modified erythrocytes exposed to t-BuOOH. Biochim. Biophys. Acta 2005;1734:74–85. [PubMed: 15866485]

Lopez-Revuelta A, Sanchez-Gallego JI, Garcia-Montero AC, Hernandez-Hernandez A, Sanchez-Yague J, Llanillo M. Membrane cholesterol in the regulation of aminophospholipid asymmetry and phagocytosis in oxidized erythrocytes. Free Radic. Biol. Med 2007;42:1106–1118. [PubMed: 17349937]

Lovell MA, Xie C, Markesbery WR. Acrolein is increased in Alzheimer's disease brain and is toxic to primary hippocampal cultures. Neurobiol. Aging 2001;22:187–194. [PubMed: 11182468]

Mandal D, Moitra PK, Saha S, Basu J. Caspase 3 regulates phosphatidylserine externalization and phagocytosis of oxidatively stressed erythrocytes. FEBS Lett 2002;513:184–188. [PubMed: 11904147]

Mandal D, Mazumder A, Das P, Kundu M, Basu J. Fas-, caspase 8-, and caspase 3-dependent signaling regulates the activity of the aminophospholipid translocase and phosphatidylserine externalization in human erythrocytes. J Biol Chem 2005;280:39460–39467. [PubMed: 16179347]

Markesbery WR, Lovell MA. 4-Hydroxynonenal, a product of lipid peroxidation, is increased in the brain in Alzheimer's disease. Neurobiol. Aging 1998;19:33–36. [PubMed: 9562500]

Martin SJ, Finucane DM, Amarante-Mendes GP, O'Brien GA, Green DR. Phosphatidylserine externalization during CD95-induced apoptosis of cells and cytoplasts requires ICE/CED-3 protease activity. J Biol Chem 1996;271:28753–28756. [PubMed: 8910516]

Martins IC, Kuperstein I, Wilkinson H, Maes E, Vanbrabant M, Jonckheere W, Van Gelder P, Hartmann D, D'Hooge R, De Strooper B, Schymkowitz J, Rousseau F. Lipids revert inert Aβ amyloid fibrils to neurotoxic protofibrils that affect learning in mice. EMBO J 2008;27:224–233. [PubMed: 18059472]

Mattson MP. Cellular actions of β-amyloid precursor protein and its soluble and fibrillogenic derivatives. Physiol. Rev 1997;77:1081–1132. [PubMed: 9354812]

Mattson MP. Pathways towards and away from Alzheimer's disease. Nature 2004;430:631–639. [PubMed: 15295589]

McGowan E, Pickford F, Kim J, Onstead L, Eriksen J, Yu C, Skipper L, Murphy MP, Beard J, Das P, Jansen K, Delucia M, Lin WL, Dolios G, Wang R, Eckman CB, Dickson DW, Hutton M, Hardy J, Golde T. Aβ42 is essential for parenchymal and vascular amyloid deposition in mice. Neuron 2005;47:191–199. [PubMed: 16039562]

McLaurin J, Chakrabartty A. Characterization of the interactions of Alzheimer β-amyloid peptides with phospholipid membranes. Eur. J. Biochem 1997;245:355–363. [PubMed: 9151964]

Mohmmad Abdul H, Butterfield DA. Protection against amyloid β-peptide (1–42)-induced loss of phospholipid asymmetry in synaptosomal membranes by tricyclodecan-9-xanthogenate (D609) and ferulic acid ethyl ester: Implications for Alzheimer's disease. Biochim. Biophys. Acta 2005;1741:140–148. [PubMed: 15955457]

Mohmmad Abdul H, Sultana R, Keller JN, St Clair DK, Markesbery WR, Butterfield DA. Mutations in amyloid precursor protein and presenilin-1 genes increase the basal oxidative stress in murine neuronal cells and lead to increased sensitivity to oxidative stress mediated by amyloid β-peptide (1–42), H_2O_2 and kainic acid: implications for Alzheimer's disease. J. Neurochem 2006;96:1322–1335. [PubMed: 16478525]

Mohmmad Abdul H, Sultana R, St Clair D, Markesbery WR, Butterfield DA. Oxidative damage in brain from human mutant *APP/PS-1* double knock-in mice as a function of age. Free Radic. Biol. Med 2008;45:1420–1425. [PubMed: 18762245]

Moses GS, Jenses MD, Lue LF, Walker DG, Sun AY, Sun GY. Secretory PLA2-IIA: a new inflammatory factor for Alzheimer's disease. J. Inflammation 2006;7:28.

Mucke L, Masliah E, Yu GQ, Mallory M, Rockenstein EM, Tatsuno G, Hu K, Kholodenko D, Johnson-Wood K, McConlogue L. High-level neuronal expression of Aβ (1–42) in wild-type human amyloid protein precursor transgenic mice: Synaptotoxicity without plaque formation. J. Neurosci 2000;20:4050–4058. [PubMed: 10818140]

Muller WE, Koch S, Eckert A, Hartmann H, Scheuer K. β-Amyloid peptide decreases membrane fluidity. Brain Res 1995;674:133–136. [PubMed: 7773681]

Murphy MP, Beckett TL, Ding Q, Patel E, Markesbery WR, St Clair DK, LeVine H 3rd, Keller JN. Aβ solubility and deposition during AD progression and in *APPxPS-1* knock-in mice. Neurobiol. Dis 2007;27:301–311. [PubMed: 17651976]

Nicholson DW, Ali A, Thornberry NA, Vaillancourt JP, Ding CK, Gallant M, Gareau Y, Griffin PR, Labelle M, Lazebnik YA, et al. Identification and inhibition of the ICE/CED-3 protease necessary for mammalian apoptosis. Nature 1995;376:37–43. [PubMed: 7596430]

Nicholson DW. Caspase structure, proteolytic substrates, and function during apoptotic cell death. Cell Death Differ 1999;6:1028–1042. [PubMed: 10578171]

Oyama F, Sawamura N, Kobayashi K, Morishima-Kawashima M, Kuramochi T, Ito M, Tomita T, Maruyama K, Saido TC, Iwatsubo T, Capell A, Walter J, Grunberg J, Ueyama Y, Haass C, Ihara Y. Mutant presenilin-2 transgenic mouse: effect on an age-dependent increase of amyloid β-protein 42 in the brain. J. Neurochem 1998;71:313–322. [PubMed: 9648880]

Paulusma CC, Oude Elferink RP. The type 4 subfamily of P-type ATPases, putative aminophospholipid translocases with a role in human disease. Biochim. Biophys. Acta 2005;1741:11–24. [PubMed: 15919184]

Poon HF, Calabrese V, Scapagnini G, Butterfield DA. Free radicals: Key to brain aging and heme oxygenase as a cellular response to oxidative stress. J. Gerontol. A. Biol. Sci. Med. Sci 2004;59:478–493. [PubMed: 15123759]

Reaume AG, Howland DS, Trusko SP, Savage MJ, Lang DM, Greenberg BD, Siman R, Scott RW. Enhanced amyloidogenic processing of the β-amyloid precursor protein in gene-targeted mice bearing the Swedish familial Alzheimer's disease mutations and a "humanized" Aβ sequence. J. Biol. Chem 1996;271:23380–23388. [PubMed: 8798542]

Sadrzadeh SM, Vincenzi FF, Hinds TR. Simultaneous measurement of multiple membrane ATPases in microtiter plates. J. Pharmacol. Toxicol. Methods 1993;30:103–110. [PubMed: 8298181]

Scheuner D, Eckman C, Jensen M, Song X, Citron M, Suzuki N, Bird TD, Hardy J, Hutton M, Kukull W, Larson E, Levy-Lahad E, Viitanen M, Peskind E, Poorkaj P, Schellenberg G, Tanzi R, Wasco W, Lannfelt L, Selkoe D, Younkin S. Secreted amyloid β-protein similar to that in the senile plaques of Alzheimer's disease is increased *in vivo* by the presenilin-1 and -2 and APP mutations linked to familial Alzheimer's disease. Nat. Med 1996;2:864–870. [PubMed: 8705854]

Schubert D, Behl C, Lesley R, Brack A, Dargusch R, Sagara Y, Kimura H. Amyloid peptides are toxic via a common oxidative mechanism. Proc. Natl. Acad. Sci. U. S. A 1995;70:1989–1993. [PubMed: 7892213]

Selkoe DJ, Yamazaki T, Citron M, Podlisny MB, Koo EH, Teplow DB, Haass C. The role of APP processing and trafficking pathways in the formation of amyloid β-protein. Ann. N. Y. Acad. Sci 1996;777:57–64. [PubMed: 8624127]

Selkoe DJ. Alzheimer's disease results from the cerebral accumulation and cytotoxicity of amyloid β-protein. J. Alzheimers. Dis 2001;3:75–80. [PubMed: 12214075]

Siman R, Reaume AG, Savage MJ, Trusko S, Lin YG, Scott RW, Flood DG. Presenilin-1 *P264L* knock-in mutation: differential effects on Aβ production, amyloid deposition, and neuronal vulnerability. J. Neurosci 2000;20:8717–8726. [PubMed: 11102478]

Snyder EM, Nong Y, Almeida CG, Paul S, Moran T, Choi EY, Nairn AC, Salter MW, Lombroso PJ, Gouras GK, Greengard P. Regulation of NMDA receptor trafficking by amyloid-β. Nat. Neurosci 2005;8:1051–1058. [PubMed: 16025111]

Sokolov Y, Kozak JA, Kayed R, Chanturiya A, Glabe C, Hall JE. Soluble amyloid oligomers increase bilayer conductance by altering dielectric structure. J. Gen. Physiol 2006;128:637–647. [PubMed: 17101816]

Sturchler-Pierrat C, Abramowski D, Duke M, Wiederhold KH, Mistl C, Rothacher S, Ledermann B, Burki K, Frey P, Paganetti PA, Waridel C, Calhoun ME, Jucker M, Probst A, Staufenbiel M, Sommer B. Two amyloid precursor protein transgenic mouse models with Alzheimer disease-like pathology. Proc. Natl. Acad. Sci. U. S. A 1997;94:13287–13292. [PubMed: 9371838]

Su JH, Zhao M, Anderson AJ, Srinivasan A, Cotman CW. Activated caspase-3 expression in Alzheimer's and aged control brain: correlation with Alzheimer pathology. Brain Res 2001;898:350–357. [PubMed: 11306022]

Tyurina YY, Tyurin VA, Zhao Q, Djukic M, Quinn PJ, Pitt BR, Kagan VE. Oxidation of phosphatidylserine: A mechanism for plasma membrane phospholipid scrambling during apoptosis? Biochem. Biophys. Res. Commun 2004;324:1059–1064. [PubMed: 15485662]

Vanags DM, Porn-Ares MI, Coppola S, Burgess DH, Orrenius S. Protease involvement in fodrin cleavage and phosphatidylserine exposure in apoptosis. J Biol Chem 1996;271:31075–31085. [PubMed: 8940103]

Westerman MA, Cooper-Blacketer D, Mariash A, Kotilinek L, Kawarabayashi T, Younkin LH, Carlson GA, Younkin SG, Ashe KH. The relationship between Aβ and memory in the Tg2576 mouse model of Alzheimer's disease. J. Neurosci 2002;22:1858–1867. [PubMed: 11880515]

Whittaker VP. Thirty years of synaptosome research. J. Neurocytol 1993;22:735–742. [PubMed: 7903689]

Wirths O, Weis J, Szczygielski J, Multhaup G, Bayer TA. Axonopathy in an APP/PS1 transgenic mouse model of Alzheimer's disease. Acta Neuropathol 2006;111:312–319. [PubMed: 16520967]
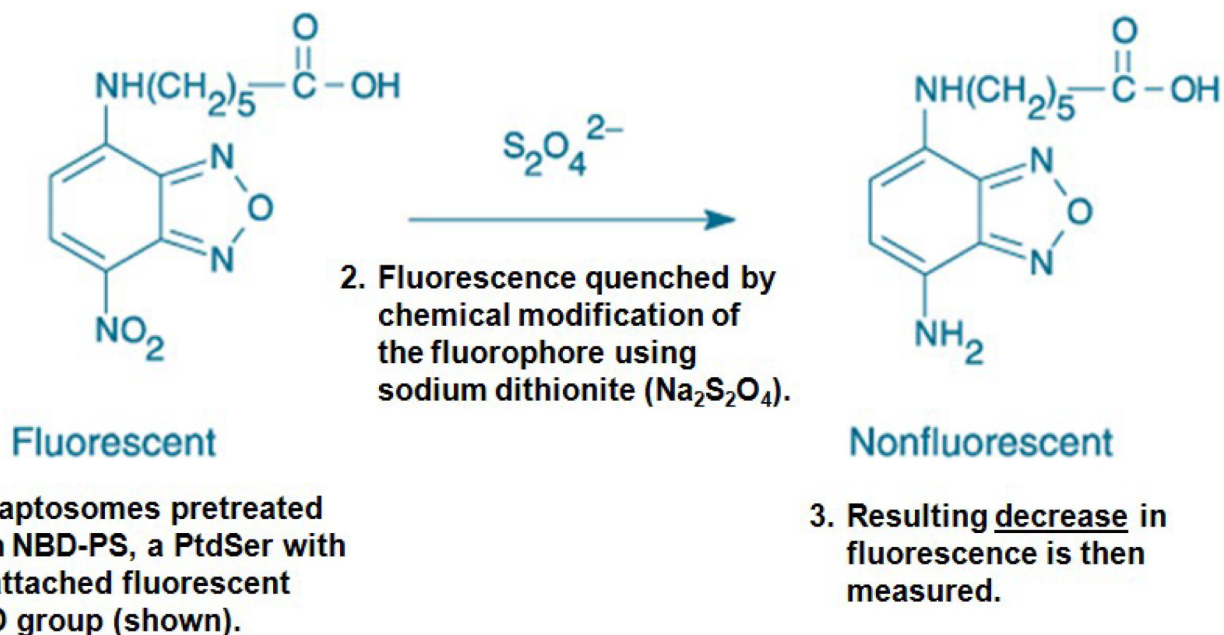
Figure 1. NBD-PS assay overview

This schematic of the NBD-PS procedure shows the chemical quenching reaction between a fluorescent NBD group attached to PtdSer and the ionic form of $Na_2S_2O_4$. Incubation of cell membranes with NBD-PS allows for probe incorporation into the inner leaflet by an active flippase enzyme. If flippase were rendered inactive, the fluorescent NBD-PS would remain exposed to the extracellular environment on the outer leaflet, where it becomes susceptible to $S_2O_4^{2-}$ quenching. In this assay, it is a significant decrease in fluorescence that is of statistical interest. However, in order to avoid graphical results showing negative values, data were analyzed as a percentage of control values set to 100%, resulting in a graphical presentation more familiar for biochemical assays.
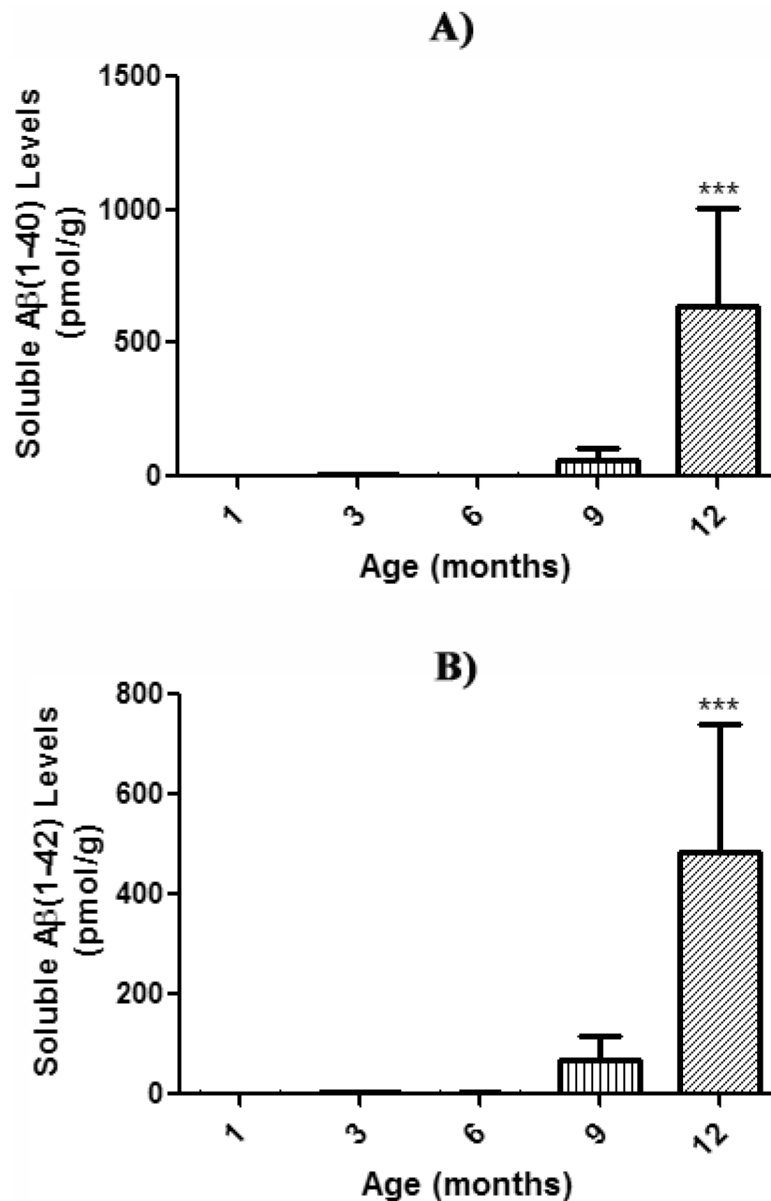
Figure 2. Soluble Aβ load in SDS-fractions of aging APP/PS-1 mouse brain
Soluble Aβ(1–40) and Aβ(1–42) levels in brain from 1, 3, 6, 9, and 12 month-old APP/PS-1
mice were quantified (pmol/g wet tissue) by two-site sandwich ELISA on SDS fractions.
Results demonstrate a significant age-dependent increase in soluble **a)** Aβ(1–40) and **b)** Aβ
(1–42) compared to respective 1 month-old APP/PS-1 controls, which suggests soluble, toxic
Aβ species could potentially induce early oxidative stress conditions and subsequent collapse
in PtdSer asymmetry. Data are presented as mean ± S.E.M. and significance assessed by one-
way ANOVA followed by a Tukey post-hoc analysis; ***P<0.001. **A)** Aβ(1–40): 1 month-
old, N=23; 3 months-old, N=5; 6 months-old, N=5; 9 months-old, N=5; 12 months-old, N=5.
B) Aβ(1–42): 1 month-old, N=23; 3 months-old, N=5; 6 months-old, N=5; 9 months-old, N=5;
12 months-old, N=5.
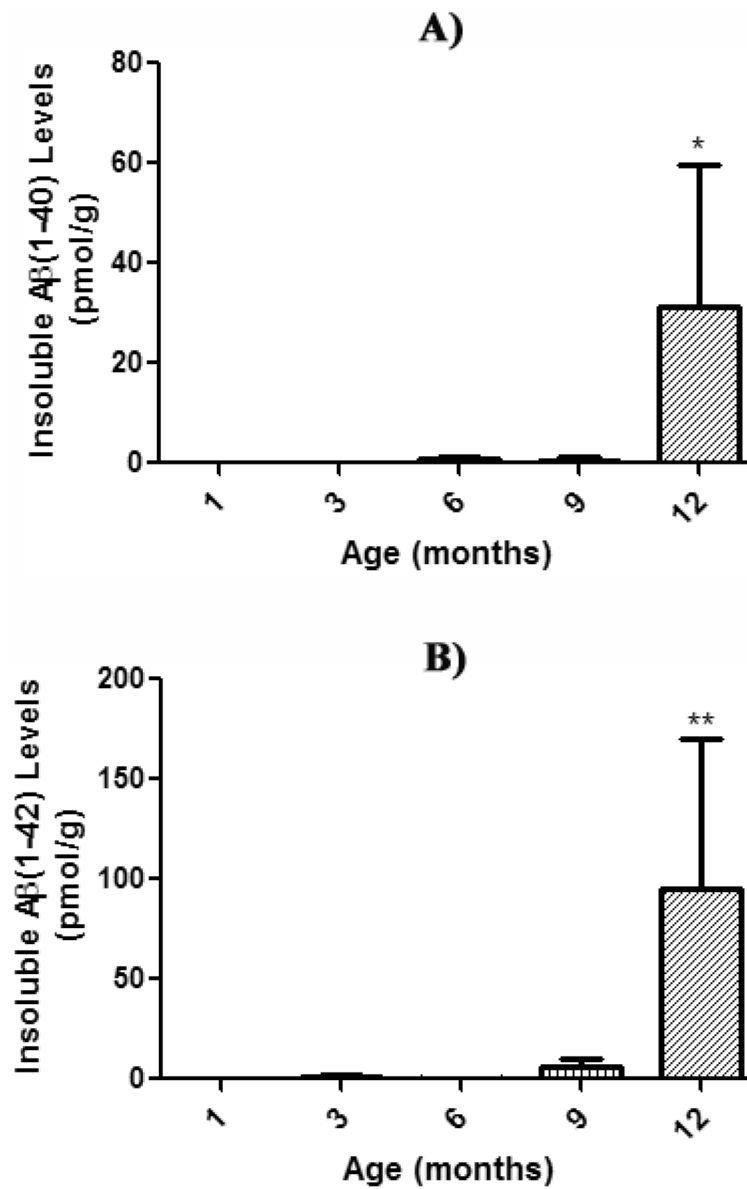
Figure 3. Insoluble Aβ load in FA-fractions of aging APP/PS-1 mouse brain

Insoluble Aβ(1–40) and Aβ(1–42) levels in brain from 1, 3, 6, 9, and 12 month-old APP/PS-1 mice were quantified (pmol/g wet tissue) by two-site sandwich ELISA on FA fractions. Results demonstrate a significant age-dependent increase in insoluble **A)** Aβ(1–40) and **B)** Aβ(1–42) compared to respective 1 month-old APP/PS-1 controls, suggesting that soluble Aβ is most likely associated with the observed age-dependent collapse in PtdSer asymmetry, and not the insoluble, plaque-deposited species. Data are presented as mean ± S.E.M. and significance assessed by one-way ANOVA followed by a Tukey post-hoc analysis; *P<0.05, **P<0.01. **A)** Aβ(1–40): 1 month-old, N=23; 3 months-old, N=5; 6 months-old, N=5; 9 months-old, N=5; 12 months-old, N=5. **B)** Aβ(1–42): 1 month-old, N=23; 3 months-old, N=5; 6 months-old, N=5; 9 months-old, N=5; 12 months-old, N=5.
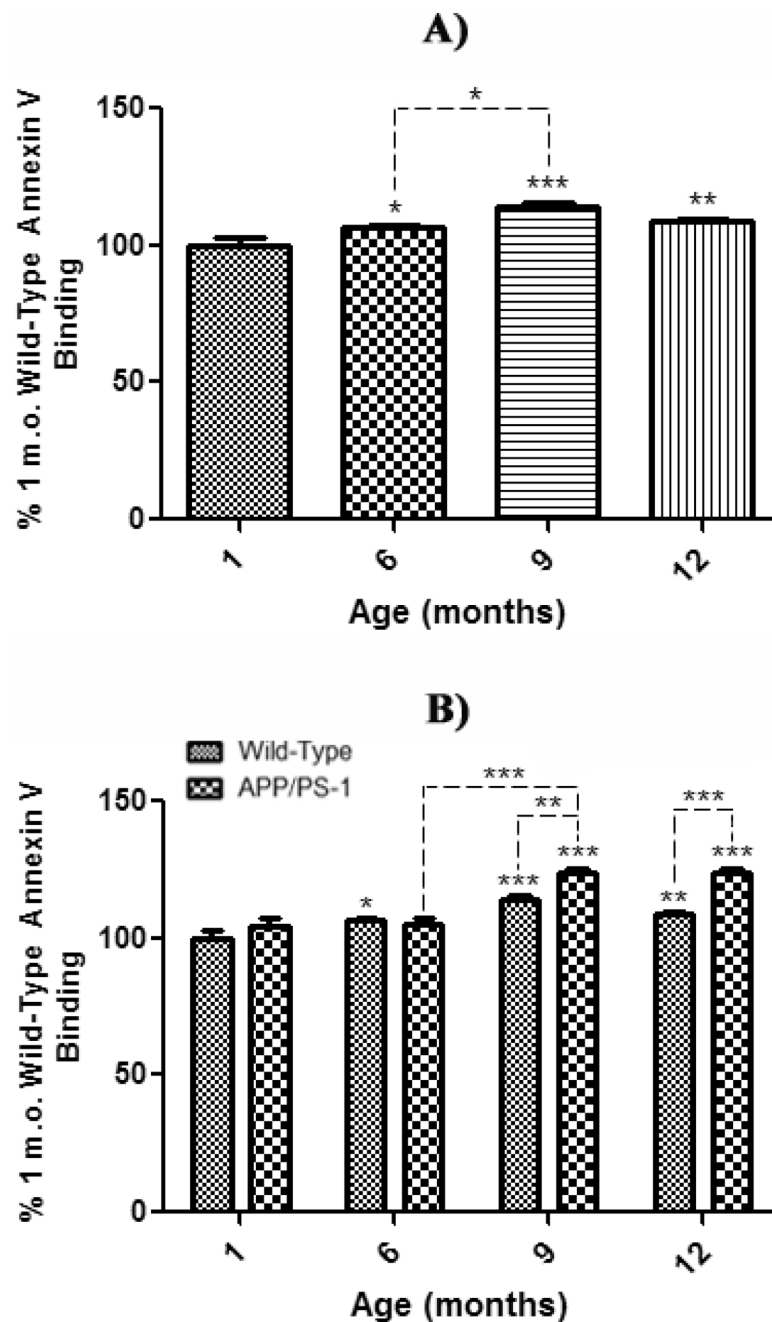
Figure 4. Annexin V binding assay in synaptosomes from wild-type and APP/PS-1 mice
Synaptosomes isolated from 1, 6, 9, and 12 month-old WT and APP/PS-1 mice were treated with the Annexin V FITC (AV). **A)** PtdSer outer leaflet exposure for each WT age-group is presented as a percentage of 1 month-old WT control. Results demonstrate a significant increase in AV fluorescence beginning at 6 months-old that continues to increase with age. Percent control values are presented as mean ± S.D. and significance assessed by one-way ANOVA followed by a Tukey post-hoc analysis; *P<0.05, **P<0.01, ***P<0.001. 1, 9, and 12 month age groups, N=5; 6 month-old, N=8. **B)** PtdSer outer leaflet exposure for each WT and APP/PS-1 age-group is presented as a percentage of 1 month-old WT control. Results demonstrate a dramatic age-dependent increase in AV fluorescence in both wild-type and APP/

PS-1 mice from 6 to 9 months-old that continues to increase with age. However, this decrease is more prominent in APP/PS-1 mice, suggesting that increasing oxidative stress, Aβ load, and/or apoptosis may cause significantly more PtdSer exposure than normal brain aging. Percent control values are presented as mean ± S.D. and significance assessed by two-way ANOVA followed by a Bonferroni post-hoc analysis; *$P<0.05$, **$P<0.01$, ***$P<0.001$. 1, 9, and 12 month age groups, N=5; 6 month-old, N=8.
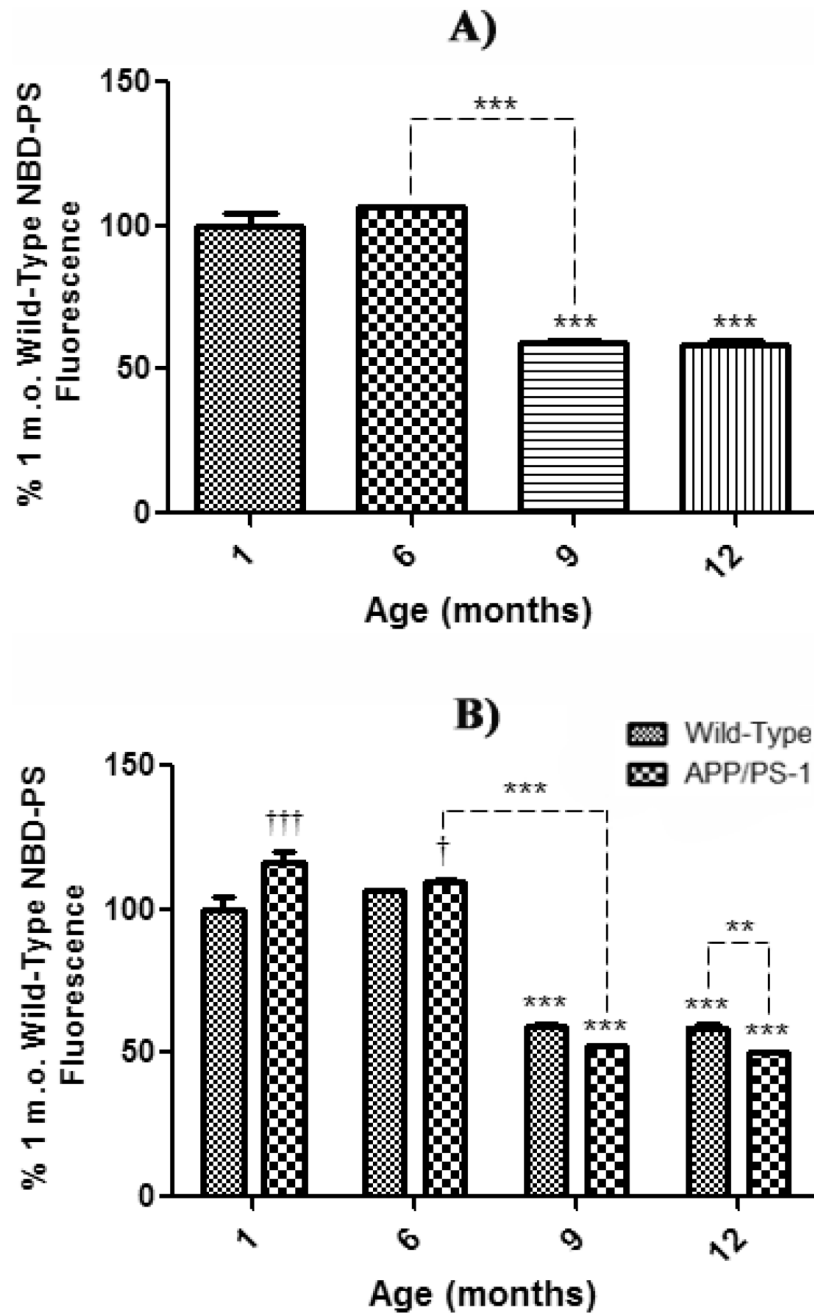
Figure 5. NBD-PS assay in synaptosomes from wild-type and APP/PS-1 mice
Synaptosomes isolated from 1, 6, 9, and 12 month-old WT and APP/PS-1 mice were treated
with the fluorescent phospholipid NBD-PS and quenched with $Na_2S_2O_4$. **A)** PtdSer outer
leaflet exposure for each WT age-group is presented as a percentage of 1 month-old WT mice
as a control. Results demonstrate a significant decrease in NBD-PS fluorescence from 6 to 9
months-old that continues to decrease with age. Percent control values are presented as mean
± S.D. and significance assessed by one-way ANOVA followed by a Tukey post-hoc analysis;
***P<0.001. 1, 9, and 12 month age groups, N=5; 6 month-old, N=8. **B)** PtdSer outer leaflet
exposure for each WT and APP/PS-1 age-group is presented as a percentage of 1 month-old
WT control. Results demonstrate a dramatic age-dependent decrease in NBD-PS fluorescence

in both WT and APP/PS-1 mice from 6 to 9 months-old. However, this decrease is more prominent in APP/PS-1 mice, suggesting that increasing oxidative stress, Aβ load, and/or apoptosis may cause significantly more PtdSer exposure than normal brain aging. Conversely, at 1 and 6 months-old there was a significant increase in APP/PS-1 fluorescence, suggesting less PtdSer exposure to the outer leaflet at these ages compared to age-matched, WT controls. Percent control values are presented as mean ± S.D. and significance assessed by two-way ANOVA followed by a Bonferroni post-hoc analysis; Significant decrease: $**P<0.01$, $***P<0.001$; Significant increase: $†P<0.05$, $††P<0.01$. 1, 9, and 12 month age groups, N=5; 6 month-old, N=8.
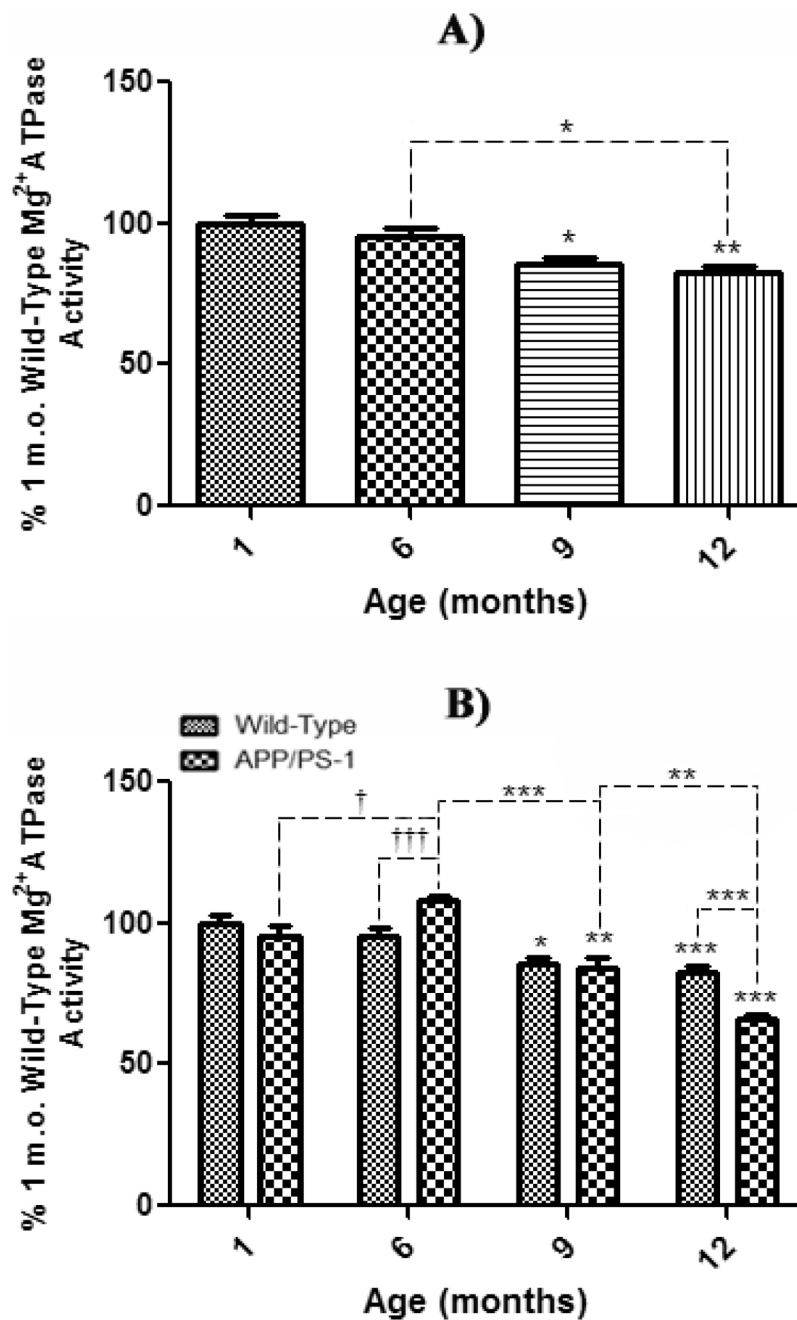
Figure 6. Mg^{2+} ATPase activity in synaptosomes from wild-type and APP/PS-1 mice
Synaptosomal Mg^{2+}ATPase activity from 1, 6, 9, and 12 month-old WT and APP/PS-1 mice was measured to represent flippase activity, an ATP-dependent, membrane-bound PtdSer translocase. Decreased UV-absorbance (810 nm) denotes decreased Mg^{2+}ATPase (i.e., flippase) activity. **A)** Mg^{2+}ATPase activity for each WT age-group is presented as a percentage of 1 month-old WT mice as a control. Results demonstrate a significant decrease in Mg^{2+}ATPase activity beginning at 9 months that continues to decrease with age. Percent control values are presented as mean ± S.D. and significance assessed by one-way ANOVA followed by a Tukey post-hoc analysis; *P<0.05, **P<0.01. 1, 9, and 12 month age groups, N=5; 6 month-old, N=8. **B)** Mg^{2+}ATPase activity for each WT and APP/PS-1 age-group is

presented as a percentage of 1 month-old WT mice as a control. Results demonstrate a significant decrease in Mg^{2+}ATPase activity beginning at 9 months that continues to decrease with age. Results demonstrate a dramatic age-dependent decrease in Mg^{2+}ATPase activity in both WT and APP/PS-1 mice from 6 to 9 months-old. However, this decrease is more prominent in APP/PS-1 mice at 12 months-old, suggesting that increasing oxidative stress, Aβ load, and/ or apoptosis may cause significantly more damage to transmembrane proteins, thus affecting PtdSer asymmetry. Conversely, from 1 to 6 months-old there was a significant increase enzyme activity in APP/PS-1 brain, suggesting significant protection or up-regulation of Mg^{2+}ATPases at these ages WT mice. Percent control values are presented as mean ± S.D. and significance assessed by two-way ANOVA followed by a Bonferroni post-hoc analysis; Significant decrease: *$P<0.05$, **$P<0.01$, ***$P<0.001$; Significant increase: †$P<0.05$, †††$P<0.001$. 1, 9, and 12 month age groups, N=5; 6 month-old, N=8.
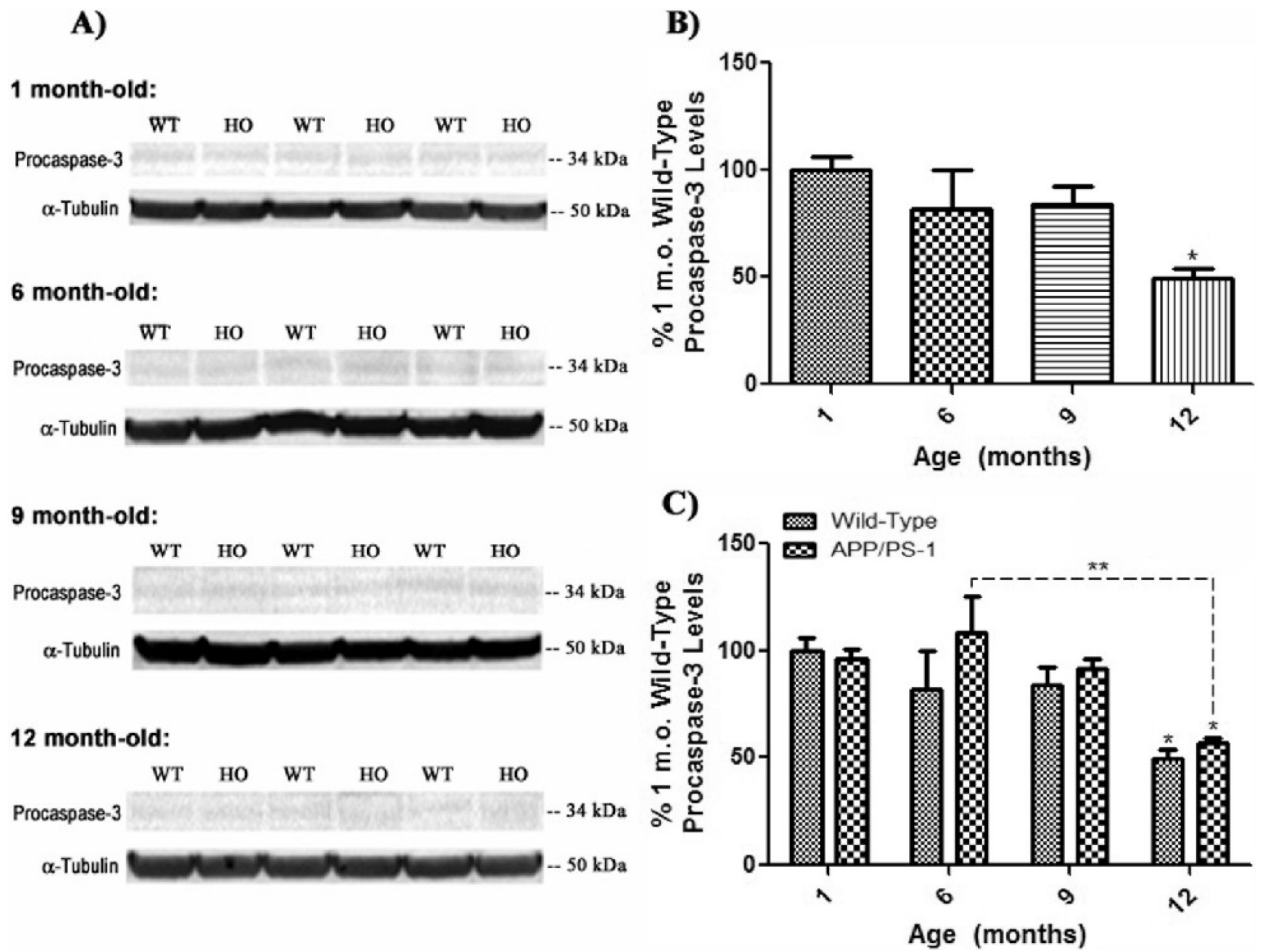
Figure 7. Procaspase-3 levels in brain from wild-type and APP/PS-1 mice
Procaspase-3 levels were measured by 1D-PAGE (75 µg/lane) and subsequent Western blot analysis in 1, 6, 9, and 12 month-old WT and APP/PS-1 mice in order to correlate decreasing flippase activity with levels of pro-apoptotic factor expression. **A)** Increased band intensity after normalization with α-tubulin represents an increase in the amount of procaspase-3 present. N=5 for all age-groups, however only representative bands from N=3 independent samples are shown. **B)** Graphical analysis of WT mouse band intensities at each age compared to 1 month-old WT mice as a control. Results demonstrate a gradual decrease in procaspase-3 levels with age that becomes significant at 12 months-old. Percent control values are presented as mean ± S.D. and significance assessed by one-way ANOVA followed by a Tukey post-hoc analysis; *P<0.05; N=5 for all age-groups. **C)** Graphical analysis of WT and APP/PS-1 (HO) band intensities at each age compared to 1 month-old WT controls. Results show that APP/PS-1 mice also present a decrease in procaspase-3 levels that becomes significant at 12 months-old. However, it appears that, like NBD-PS data, there is an obvious increase in 6 month-old APP/PS-1 procasepase-3 levels, although not significant, suggesting a possible increase in apoptotic processes at this early age compared to WT mice. Percent control values are presented as mean ± S.D. and significance assessed by two-way ANOVA followed by a Bonferroni post-hoc analysis; *P<0.05, **P<0.01; N=5 for all age-groups.
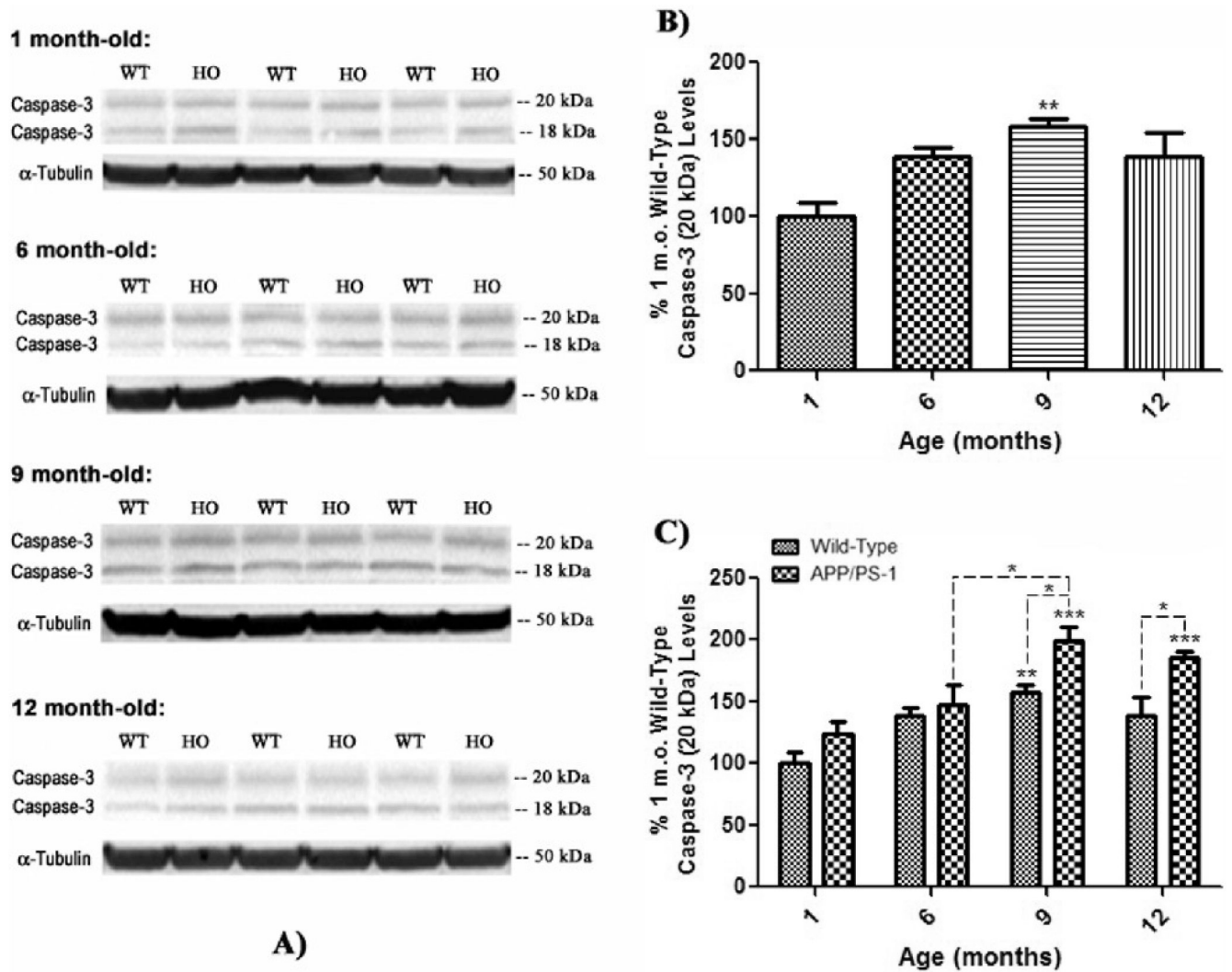
Figure 8. Active p18 fragment caspase-3 levels in brain from wild-type and APP/PS-1 mice
Active caspase-3 fragment, p18 (20 kDa) levels were measured by 1D-PAGE (75 µg/lane) and subsequent Western blot analysis in 1, 6, 9, and 12 month-old WT and APP/PS-1 mice in order to correlate decreasing flippase activity with levels of pro-apoptotic factor expression. **A)** Increased band intensity after normalization with α-tubulin represents an increase in the amount of the p18 caspase-3 fragment present. Wild-type, WT; APP/PS-1, HO. N=5 for all age-groups, however only representative bands from N=3 independent samples are shown. **B)** Graphical analysis of WT mouse band intensities at each age compared to 1 month-old WT mice as a control. Results demonstrate a gradual increase in p18 levels with age that becomes significant at 9 months-old. Percent control values are presented as mean ± S.D. and significance assessed by one-way ANOVA followed by a Tukey post-hoc analysis; **$P<0.01$; N=5 for all age-groups. **C)** Graphical analysis of WT and APP/PS-1 (HO) band intensities at each age compared to 1 month-old WT controls. Results show that levels of p18 in APP/PS-1 brain also significantly increase from 6 to 9 months of age. However, this age-related increase is more prominent in APP/PS-1 mice, suggesting that increasing oxidative stress and/or Aβ load may cause significantly more apoptosis than normal brain aging. Percent control values are

presented as mean ± S.D. and significance assessed by two-way ANOVA followed by a Bonferroni post-hoc analysis; *P<0.05, **P<0.01, ***P<0.001; N=5 for all age-groups.
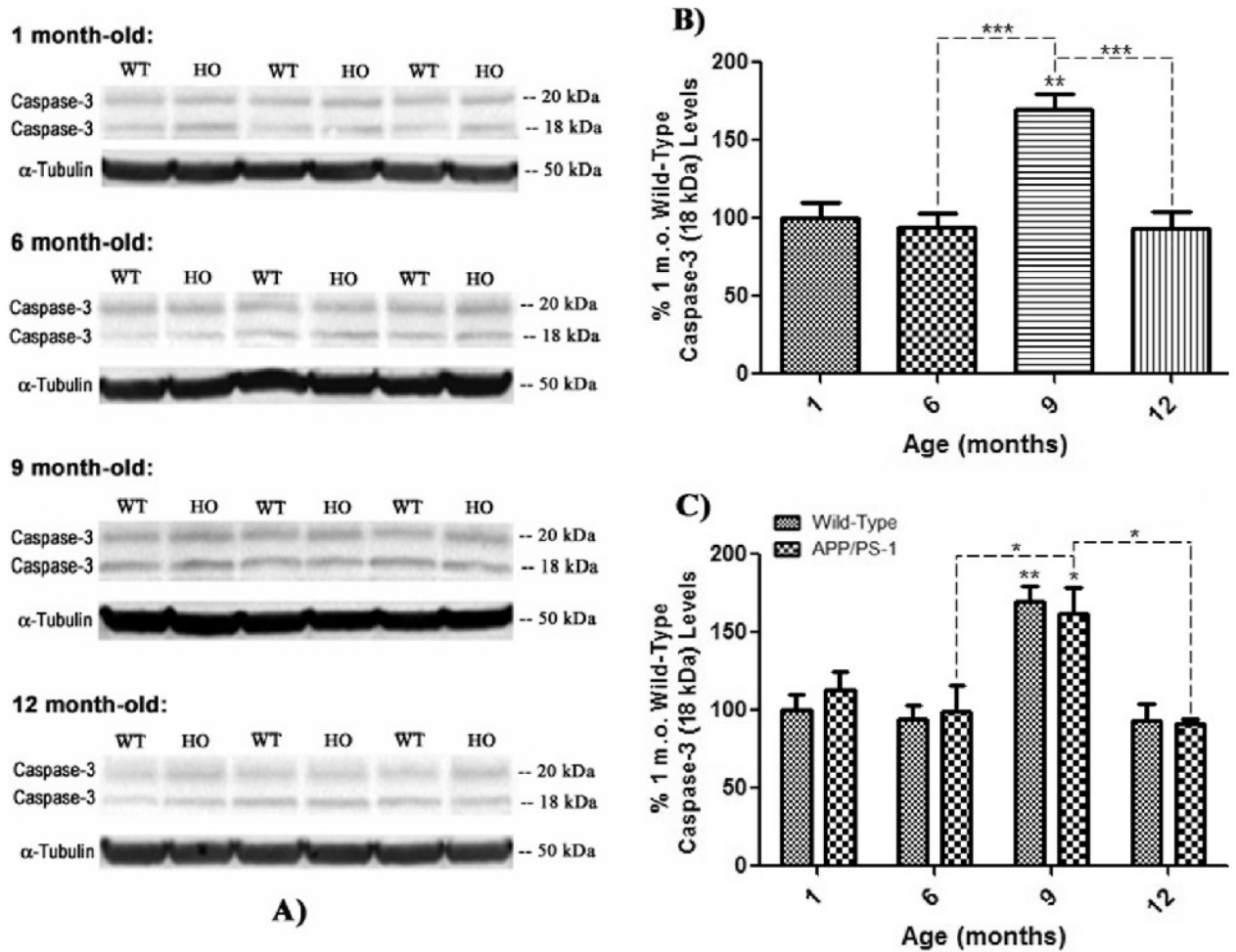
Figure 9. Active p12 fragment caspase-3 levels in brain from wild-type and APP/PS-1 mice
Active caspase-3 fragment, p12 (18 kDa) levels were measured by 1D-PAGE (75 µg/lane) and subsequent Western blot analysis in 1, 6, 9, and 12 month-old WT and APP/PS-1 mice in order to correlate decreasing flippase activity with levels of pro-apoptotic factor expression. **A)** Increased band intensity after normalization with α-tubulin represents an increase in the amount of the p12 caspase-3 fragment present. Wild-type, WT; APP/PS-1, HO. N=5 for all age-groups, however only representative bands from N=3 independent samples are shown. **B)** Graphical analysis of WT mouse band intensities at each age compared to 1 month-old WT mice as a control. Results demonstrate a gradual increase in p12 levels with age that becomes significant at 9 months-old. Percent control values are presented as mean ± S.D. and significance assessed by one-way ANOVA followed by a Tukey post-hoc analysis; **P<0.01; N=5 for all age-groups. **C)** Graphical analysis of WT and APP/PS-1 (HO) band intensities at each age compared to 1 month-old WT controls. Results show that levels of p12 in APP/PS-1 brain also significantly increase from 6 to 9 months of age. However, this age-related increase is more prominent in APP/PS-1 mice, suggesting that increasing oxidative stress and/or Aβ load may cause significantly more apoptosis than normal brain aging. Percent control values are presented as mean ± S.D. and significance assessed by two-way ANOVA followed by a Bonferroni post-hoc analysis; *P<0.05, **P<0.01, ***P<0.001; N=5 for all age-groups.